

Constraint programming model and biased random-key genetic algorithm for the single-machine coupled task scheduling problem with exact delays to minimize the makespan

Vítor A. Barbosa^a, Rafael A. Melo^{a,*}

^a*Institute of Computing, Universidade Federal da Bahia, Salvador, BA 40170-115, Brazil*

Abstract

We consider the strongly NP-hard single-machine coupled task scheduling problem with exact delays to minimize the makespan. In this problem, a set of jobs has to be scheduled, each composed of two tasks interspersed by an exact delay. Given that no preemption is allowed, the goal consists of minimizing the completion time of the last scheduled task. We model the problem using constraint programming (CP) and propose a biased random-key genetic algorithm (BRKGA). Our CP model applies well-established global constraints. Our BRKGA combines some successful components in the literature: an initial solution generator, periodical restarts and shakes, and a local search algorithm. Furthermore, the BRKGA's decoder is focused on efficiency rather than optimality, which accelerates the solution space exploration. Computational experiments on a benchmark set containing instances with up to 100 jobs (200 tasks) indicate that the proposed BRKGA can efficiently explore the problem solution space, providing high-quality approximate solutions within low computational times. It can also provide better solutions than the CP model under the same computational settings, i.e., three minutes of time limit and a single thread. The CP model, when offered a longer running time of 3600 seconds and multiple threads, significantly improved the results, reaching the current best-known solution for 90.56% of these instances. Finally, our experiments highlight the importance of the shake and local search components in the BRKGA, whose combination significantly improves the results of a standard BRKGA.

Keywords: Metaheuristics, Scheduling with exact delays, Constraint programming, BRKGA, Local search

1. Introduction

The coupled-task scheduling problem (CTSP) consists of scheduling jobs, each with at least two coupled tasks. In each job, the succeeding task must be started after the preceding task is finished, with an exact delay between them. According to [Khatami et al. \(2020\)](#), there are several possible performance criteria for the CTSP. However, the major performance criteria adopted in the literature include the makespan, total completion time, maximum lateness, and earliness and tardiness. For this work, we tackle the single-machine version of the problem, where each job has two tasks that must be separated

*Corresponding author

Email addresses: vitor.barbosa@ufba.br (Vítor A. Barbosa), rafael.melo@ufba.br (Rafael A. Melo)

by an exact delay. The goal consists of minimizing the makespan. Such minimization is challenging because tasks can be scheduled within the exact delay of a job, whether by nesting jobs between other job tasks or by interleaving tasks of different jobs. Henceforth, there must be several non-singleton jobs, i.e., jobs with exact delays larger than their processing times. Otherwise, these jobs can be randomly appended at the end of a schedule without loss of generality (Li and Zhao, 2007).

Applications of the CTSP include pulsed radar systems in which a radar transmits a pulse and receives its reflection to keep track of targets (Shapiro, 1980), chemistry manufacturing processes (Aggeev and Baburin, 2007), patient appointments in medical services (Pérez et al., 2011; Condotta and Shakhlevich, 2014; Liu et al., 2019), among others. Another potential application involves the scheduling of tasks operated by robots in smart homes, especially in smart kitchens (Sharma and Reddy, 2025). In this scenario, kitchen robots (Mepani et al., 2022; Jiang and Zhou, 2022) can take advantage of idle moments between sub-tasks to perform other sub-tasks, thus reducing the total preparation time (Bautista et al., 2023; Yi et al., 2022). Yi et al. (2022) studied a similar problem involving multiple tasks operated by dual-arm kitchen robots in a controlled environment.

The single machine coupled-task scheduling problem (SMCTSP) to minimize makespan is classified as a strongly NP-hard problem (Orman and Potts, 1997; Sherali and Smith, 2005). Condotta and Shakhlevich (2012) showed that obtaining an optimal solution is NP-hard even if there is a predefined sequence for the initial (or final) tasks and all the jobs have unit processing times. Li and Zhao (2007) proposed a tabu-search heuristic for the SMCTSP. Hwang and Lin (2011) studied the SMCTSP with fixed-job-sequence, i.e., if job A precedes job B , then the initial and final tasks of job A must precede the initial and final tasks of job B , respectively. The authors designed an $O(n^2)$ algorithm to schedule with minimum makespan a given task sequence abiding by the fixed-job-sequence constraint, in addition to determining its feasibility. Bessy and Giroudeau (2019) recently investigated the parameterized complexity of the CTSP. Khatami et al. (2020) presented a comprehensive review of the different types of CTSP. They also presented mixed integer programming (MIP) formulations for several coupled scheduling problems. Khatami and Salehipour (2021) presented a binary search-based MIP heuristic, in addition to some lower and upper bounds. Békési et al. (2022) provided an approximation algorithm for a special case in which jobs only have two different delay times. Recently, Khatami and Salehipour (2024) proposed a new IP formulation and a relax-and-solve heuristic for the SMCTSP, which, to the best of our knowledge, is the current state-of-the-art method. We refer to Khatami et al. (2020) for a literature survey on coupled task scheduling problems.

The main contributions of our work are highlighted in the following. First, we propose a constraint programming (CP) model that outperforms all the state-of-the-art approaches, both exact and heuristic methods. Second, we devise a BRKGA metaheuristic, denoted as BRKGA-R-S-LS, that can efficiently explore the solution space and find high-quality solutions in low computational times. Besides, it outperforms the CP model when both are run under the same computational settings, i.e., a low time limit and a single thread. It is worth highlighting that we considered the 240 instances available from the literature, which have instances with up to 100 jobs (200 coupled tasks) (Khatami et al., 2019, 2020). Over them, the CP model obtained 71 optimal solutions. Considering the solutions obtained in this paper, there are 73 optimal solutions in total.

Our BRKGA-R-S-LS stands for *Biased Random-Key Genetic Algorithm with Restarts, Shakes and Local Search*, and combines some successful components in the literature: an initial solution generator, periodical restarts and shakes, and a local search procedure. The initial solution generator aims to provide the competitive advantage of starting the search guided by good solutions. The restarts and shakes intend to direct the search to new paths, whether completely different (restart) or similar (shake). Finally, the objective of the local search is to assist the intensification mechanism of the search. The BRKGA-R-S-LS is also compared to a standard BRKGA with an initial solution generator restarts, denoted as BRKGA-R, to analyze the impact of the shake and local search on solution quality.

1.1. Constraint programming motivation

CP is a computational paradigm for solving a constraint satisfaction problem (CSP) (Rossi et al., 2006). A CSP is represented in terms of decision variables and the relations that must hold among them, i.e., the constraints. A constraint solver takes one CSP instance and assigns a value for each variable while satisfying the problem constraints. When a feasible solution is achieved, the solver propagates the constraints to prune the search space, reducing the domain of the variables. Besides, each constraint solver applies dedicated algorithms for exploiting the structure and properties of the constraint.

Note that CP is focused on feasibility rather than optimality. Nevertheless, CP can also be used to find an optimal solution for optimization CSPs by solving a sequence of CSPs. Therefore, the constraint solver will initially find a feasible solution for the problem with a value. Then, it imposes a constraint that the next solution must be better. Whenever the solver fails to find a feasible solution, the previous solution is optimal. Although CP can take too long in practice, it is guaranteed to find an optimal solution. Additionally, it has been demonstrated to be a strong approach for scheduling problems, because the new constraint reduces the search space.

The reason to apply CP to the SMCTSP is its potential success over scheduling problems in the past years. For instance, Lunardi et al. (2020) devised CP models for the online printing shop scheduling problem, solving to optimality all small-sized and a fraction of the medium-sized instances, in addition to providing feasible solutions for large-sized instances that appear in practice. Da Col and Teppan (2022) showed that CP can also be efficiently applied to industrial-size job scheduling problems, dealing with instances with up to one million operations. Awad et al. (2022) demonstrated the success of their CP model to minimize the makespan of a large scheduling problem in batch pharmaceutical manufacturing facilities.

1.2. Biased random-key genetic algorithm motivation

The BRKGA is a population-based search metaheuristic proposed by Gonçalves and Resende (2011) that simplifies genetic algorithms by making the solution representation aspects and the intensification-diversification mechanism problem independent. Such simplification led the BRKGA to be successfully applied to several combinatorial optimization problems. Besides, the structure supports hybridization with other optimization methods in different scenarios.

Recently, Melo et al. (2023) and Silva et al. (2024) devised BRKGAs to obtain high-quality solutions in low computational times to the minimum quasi-clique partitioning problem and the Grundy coloring problem, respectively. Reixach et al. (2025) proposed a BRKGA hybridized with a beam search from

the literature to the longest common square subsequence problem, outperforming former state-of-the-art methods with statistical significance. [Chaves et al. \(2024\)](#) developed an adaptive BRKGA for the tactical berth allocation problem, which was competitive with the current state-of-the-art methods and could find the best-known solutions for most tested instances. Concerning scheduling problems, nearly one-third of all BRKGA applications are dedicated to this category of problems, making it the most extensively studied category using this metaheuristic ([Londe et al., 2025](#)).

In the context of hybridization, one or multiple heuristics can be applied to BRKGA to provide one or multiple initial solutions. This type of solution is included in the initial population and must meet some quality criterion. [Martarelli and Nagano \(2020\)](#) and [Silva et al. \(2023\)](#) showed that this strategy indicated a positive influence on the performance of the BRKGA, given the competitive advantage of starting the search guided by good solutions. Another hybridization involves employing a local search heuristic, which performs consecutive minor changes on a solution. These minor changes, called *moves*, are limited by the type of operation defined a priori, i.e., there is a constrained set of solutions to be reached, which we call *neighborhood*. Given that each move must improve the current solution, the search finishes when no possible move results in an improvement. At this point, the solution is called a local optimum. The local search heuristic can be applied in several scenarios. For instance, [Silva et al. \(2025\)](#) executed the local search after an improvement in some individuals of the elite set, while [de Abreu et al. \(2022\)](#) applied the local search only on selected iterations.

Thereupon, the motivation behind the application of the BRKGA to the SMCTSP relies on its success over scheduling problems. More specifically, the single machine coupled-task scheduling problem is constrained, considering that it imposes an exact delay between the tasks of the jobs, and the BRKGA can always decode feasible solutions with low computational effort. Furthermore, once a solution is decoded, no manipulation is necessary since the BRKGA will independently deal with the intensification and diversification mechanisms. Finally, its hybridization with the local search generally yields a positive impact on scheduling problems. We refer the reader to [Londe et al. \(2024\)](#) and [Londe et al. \(2025\)](#) for recent literature surveys about the BRKGA.

1.3. Organization

The remainder of this paper is organized as follows. Section 2 presents the notations used and the CP model. Section 3 describes the components of the proposed BRKGA-R-S-LS metaheuristic. Section 4 reports the results obtained from a series of computational experiments on the proposed methods. Section 5 concludes the paper with some final remarks.

2. Notations and constraint programming model

Consider a set of jobs $J = \{1, \dots, n\}$. Each job $j \in J$ is represented by (a_j, L_j, b_j) , where $a_j \in \mathbb{Z}_{\geq 0}$ and $b_j \in \mathbb{Z}_{\geq 0}$ denote the processing times of their initial and final tasks, respectively. $L_j \in \mathbb{Z}_{\geq 0}$ provides the exact interval between the two tasks of job j . Preemption is not allowed, and the objective is to minimize the makespan C_{max} , i.e., the completion time of the last scheduled job. Considering standard scheduling classifications, the problem can be denoted as $1|(a_j, L_j, b_j)|C_{max}$, where 1 indicates a single machine, (a_j, L_j, b_j) provides the jobs' characteristics, and C_{max} defines the objective function. It is

assumed that processing times and intervals between tasks are integer values. Additionally, denote the set of tasks by $T = \{1, \dots, 2n\}$, where tasks $2j - 1$ and $2j$ identify the initial and final tasks of job $j \in J$, respectively. Let p_h denote the processing time of task $h \in T$. Figure 1 illustrates the single machine coupled task scheduling problem along with its notations.

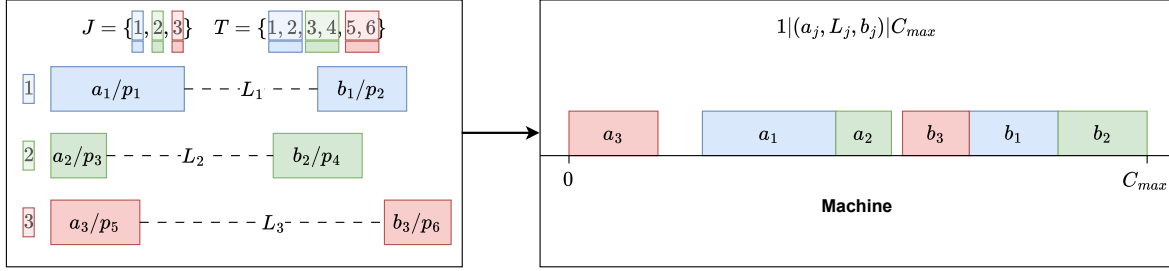


Figure 1: Illustration of the single machine coupled task scheduling problem

Define the variable s_h to represent the start time of task $h \in T$. Let the variable C_{max} indicate the completion time of the last scheduled task. Denote by UB an upper bound for C_{max} , which a possibility is to define as $UB = \sum_{j \in J} (a_j + L_j + b_j)$. The problem can be formulated as the following CP model:

$$\min C_{max} \quad (1)$$

$$s_{2j} = s_{2j-1} + p_{2j-1} + L_j, \quad \forall j \in J, \quad (2)$$

$$\text{noOverlap}(\{s_h | h \in T\}, \{p_h | h \in T\}), \quad (3)$$

$$C_{max} = \max_{h \in T} (s_h + p_h), \quad (4)$$

$$s_h \in [0, UB], \quad \forall h \in T, \quad (5)$$

$$C_{max} \in [0, UB]. \quad (6)$$

The objective function (1) minimizes the completion time of the last scheduled task, i.e., the makespan. Constraints (2) ensure the exact interval between the two tasks of each job. The global constraint $\text{noOverlap}(A, B)$ in Constraint (3) ensures that the tasks in T do not overlap, in which the starting times $A = \{s_h | h \in T\}$ and their respective processing times $B = \{p_h | h \in T\}$ represent the intervals $[s_h, s_h + p_h]$, $h \in T$, that must be disjoint. It is noteworthy that the method $\text{noOverlap}(A, B)$ can be initially modeled as a conjunction of non-overlap constraints, but can also be modeled differently depending on the underlying solver. Constraint (4) defines the makespan as the completion time of the last task. Constraints (5)-(6) define the domains of the decision variables as integer values in the specified intervals.

3. Biased random-key genetic algorithm

The BRKGA is based on the concept of Genetic Algorithms (GAs), where each problem's solution is an individual within a population, and its solution value is denoted as *fitness*. Based on the random-key genetic algorithm (RKGA) of Bean (1994), the solutions are encoded into vectors of real numbers generated randomly in the interval $[0, 1]$, these numbers being denoted keys. In each iteration of the

BRKGA, the current population generation is decoded using a deterministic algorithm, referred to as decoder, sorted by fitness, and partitioned into two subsets: elite and non-elite. The elite set contains the individuals with the best fitness, while the non-elite set comprises the remaining solutions.

The intensification mechanism in a BRKGA comprises the crossover process within the creation of a new generation of solutions. In this process, one of the parents is always an elite solution, defined as one with a high fitness value. In our case, the fitness value can be defined as a negative makespan. Moreover, the elite parent has a greater probability of passing on its characteristics, i.e., keys, to the new population. The BRKGA uses the parametric uniform crossover strategy (Spears and De Jong, 1991) to combine parent solutions and generate a new one.

For diversification, with each new iteration, the BRKGA adds a set of randomly generated solutions, called mutants, to the population. Furthermore, a BRKGA approach can allow restarts, i.e., a new initial population is generated from which the algorithm must continue generating solutions. The BRKGA can also incorporate a shake operation (Andrade et al., 2019), which perturbs all individuals from the elite set and resets the remaining population.

In this work, we propose a BRKGA that combines some successful methods in the literature: an initial solution generator, periodical restarts or shakes, and a local search. It is denoted henceforth as BRKGA-R-S-LS. To highlight the importance of a shaking operation combined with a local search, we compare it with a standard BRKGA with an initial solution generator and restarts, which we denote as BRKGA-R.

Throughout this section, we describe each component used in BRKGA-R-S-LS, namely: the encoding and the decoder (Section 3.1); the initial solution generator (Section 3.2); the local search (Section 3.3); and the perturbation (Section 3.4). At the end of the section, we detail the overall framework (Section 3.5).

3.1. Encoding and decoder

In our approach, each solution is encoded as a vector X composed of $|J|$ random keys, in which the j -th key corresponds to the job $j \in J$.

Our decoder is a polynomial-time heuristic in which the keys are used to define a sorted sequence of the jobs $\sigma^{jobs} = (\sigma_1^{jobs}, \sigma_2^{jobs}, \dots, \sigma_n^{jobs})$, where σ_k^{jobs} , $k \in \{1, \dots, n\}$, is the k -th job in the sequence. The job σ_k^{jobs} is thus inserted into the solution after the finish of the initial task of σ_{k-1}^{jobs} in the earliest possible time without overlapping with those jobs already scheduled (first-fit position). By construction, our first-fit algorithm is injective, i.e., given two different sorted sequences of the jobs, the resulting solutions are also different. On the other hand, our decoder is not injective because two random-key vectors can produce the same sorted sequence of the jobs. Figure 2 illustrates a decoding.

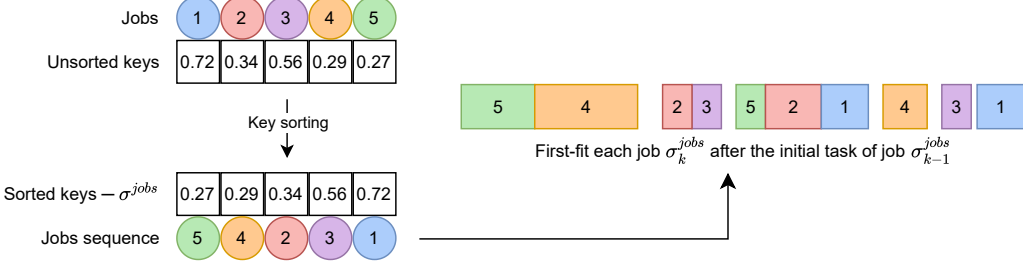


Figure 2: Decoder example.

3.1.1. Notations and main data structures for the decoder

The decoder algorithm uses the following notations and data structures, which are summarized in Table 1. Let the tuple $S : \langle \tau, \sigma^{tasks}, C_{max} \rangle$ represent a solution for the SMCTSP. Each solution S contains the following structure: $S.\tau$ is an array of integers of length $|T|$ in which $S.\tau_h$ defines the start time of the task $h \in T$ in S ; $S.\sigma^{tasks}$ is an array of integers of length $|T|$ in which $S.\sigma_i^{tasks}$, $i \in \{1, \dots, |S.\sigma^{tasks}|\}$ is the i -th task of the schedule in S ; and $S.C_{max}$ is the makespan of S .

Our decoder iteratively inserts pairs of tasks (jobs) in the schedule $S.\sigma^{tasks}$. Therefore, each pair of positions to insert a job is called an insertion candidate. This insertion candidate has a specific structure, further used to update S . Let the tuple $\mathcal{C} : \langle j, F, pos_{t_1}, pos_{t_2}, st, cost \rangle$ be an insertion candidate for a specific job. Each insertion candidate \mathcal{C} for a job $j \in J$ contains the following structure: $\mathcal{C}.j$ is the id of the job to be inserted; $\mathcal{C}.F$ is a boolean variable that indicates its feasibility; $\mathcal{C}.pos_{t_1}$ and $\mathcal{C}.pos_{t_2}$ define the insertion position of the initial and final tasks of $\mathcal{C}.j$, respectively; $\mathcal{C}.st$ defines j 's start time; $\mathcal{C}.cost$ defines its cost, which is given by the difference between the new and current values of $S.C_{max}$. It is worth mentioning that when $\mathcal{C}.pos_{t_1} = \mathcal{C}.pos_{t_2}$, the whole job $\mathcal{C}.j$ is inserted between the tasks $\mathcal{C}.\sigma_{pos_{t_1}-1}^{tasks}$ and $\mathcal{C}.\sigma_{pos_{t_1}}^{tasks}$. Additionally, if $\mathcal{C}.pos_{t_h} = |S.\sigma^{tasks}| + 1$, then the respective task $h \in \{1, 2\}$ (initial or final task) is inserted at the end of the schedule $S.\sigma^{tasks}$.

Table 1: Summary of the notation used in the decoder

Structure	Definition	Notation	Definition
S	solution	$S.\tau$ $S.\sigma^{tasks}$ $S.C_{max}$	array of the task start times of S array of the sequence of tasks in S makespan of S
\mathcal{C}	insertion candidate	$\mathcal{C}.j$ $\mathcal{C}.F$ $\mathcal{C}.pos_{t_1}$ $\mathcal{C}.pos_{t_2}$ $\mathcal{C}.st$ $\mathcal{C}.cost$	job id true if \mathcal{C} is feasible, false otherwise insert position for the initial task insert position for the final task start time of the job $\mathcal{C}.j$ cost of \mathcal{C}

3.1.2. First-fit algorithm

Algorithm 1 details the first-fit algorithm. It receives as input the insertion sequence of the jobs σ^{jobs} and the instance data I . The instance data I contains the parameters presented in Section 2. In line 1, a partial solution S is initiated with the job σ_1^{jobs} scheduled at time 0, i.e., as early as possible. In line 2, we define a variable $\overleftarrow{pos}_{t_1}$ that stores the position of the last initial task inserted in $S.\sigma^{tasks}$, i.e., $\overleftarrow{pos}_{t_1} = 1$ because the initial task of job σ_1^{jobs} was inserted in the first position of $S.\sigma^{tasks}$ (line 1). In the for loop of lines 3-17, we iteratively insert the remaining jobs of the sequence

σ_i^{jobs} (line 3) into the schedule of the solution S . In line 4, we define the job to be inserted as the job σ_i^{jobs} . In line 5, we define a dummy infeasible insertion candidate \mathcal{C}^* to serve as a sentinel. In line 6, we define another variable $post_1$ that stores the expected position of the initial task of job σ_i^{jobs} . By definition, $post_1 \geq \overleftarrow{post}_1 + 1$ because the job σ_i^{jobs} must be inserted after the finish of the initial task of job σ_{i-1}^{jobs} . In the loop of lines 7-9, we iteratively search for the first-fit insertion candidate \mathcal{C}^* when inserting the initial task of job σ_i^{jobs} at position $post_1 \leq |S.\sigma^{tasks}|$ (line 7). In line 8, the function ANALYZE_INSERTION_CANDIDATE, described in Algorithm 2, analyzes the insertion candidate's feasibility, cost, and final task's position, assuming that the initial task is placed in position $post_1$. In line 9, we increment the variable $post_1$. At the end of the loop of lines 7-9, the variable \mathcal{C}^* can be either an infeasible or a feasible insertion candidate. If it is infeasible (line 10), the job σ_i^{jobs} can only be inserted in the position $post_1 = |S.\sigma^{tasks}| + 1$ with cost $a_j + L_j + b_j$ (line 11). After that, the variable \mathcal{C}^* is a feasible insertion candidate and we can update the solution S . In lines 12 and 13, we store the start times of the initial and final tasks of the job j in the array $S.\tau$, respectively. In lines 14 and 15, we execute a function `insert(A, P, E)`, which inserts the integer E in the position P of the array A . Given that both $\mathcal{C}^*.post_1$ and $\mathcal{C}^*.post_2$ are positions in the currently unmodified schedule $S.\sigma^{tasks}$, the order of insertion matters. Consequently, we first insert the final task (line 14), then the initial task (line 15). In line 16, we update the solution makespan $S.C_{max}$ by adding the cost $\mathcal{C}^*.cost$. In line 17, the variable \overleftarrow{post}_1 is updated to $\mathcal{C}^*.post_1$. Finally, the algorithm returns the solution S in line 18.

Algorithm 1: FIRST_FIT_ALGORITHM(σ^{jobs}, I)

```

1  $S \leftarrow$  Partial solution with job  $\sigma_1^{jobs}$  scheduled at time 0;
2  $\overleftarrow{post}_1 \leftarrow 1$ ;
3 for  $i \leftarrow 2$  to  $n$  do
4    $j \leftarrow \sigma_i^{jobs}$ ;
5    $\mathcal{C}^* \leftarrow \mathcal{C} : (j, \text{false}, -, -, -, -)$ ;
6    $post_1 \leftarrow \overleftarrow{post}_1 + 1$ ;
7   while  $\mathcal{C}^*.F = \text{false}$  and  $post_1 \leq |S.\sigma^{tasks}|$  do
8      $\mathcal{C}^* \leftarrow \text{ANALYZE\_INSERTION\_CANDIDATE}(j, post_1, S, I)$ ;
9      $post_1 \leftarrow post_1 + 1$ ;
10    if  $\mathcal{C}^*.F = \text{false}$  then
11       $\mathcal{C}^* \leftarrow \mathcal{C} : (j, \text{true}, post_1, post_1, S.C_{max}, a_j + L_j + b_j)$ ;
12       $S.\tau_{2j-1} \leftarrow \mathcal{C}^*.st$ ;
13       $S.\tau_{2j} \leftarrow \mathcal{C}^*.st + a_j + L_j$ ;
14       $\text{insert}(S.\sigma^{tasks}, \mathcal{C}^*.post_2, 2j)$ ;
15       $\text{insert}(S.\sigma^{tasks}, \mathcal{C}^*.post_1, 2j - 1)$ ;
16       $S.C_{max} \leftarrow S.C_{max} + \mathcal{C}^*.cost$ ;
17       $\overleftarrow{post}_1 \leftarrow \mathcal{C}^*.post_1$ ;
18 return  $S$ ;

```

Algorithm 2 describes the pseudocode for the ANALYZE_INSERTION_CANDIDATE invoked in line 8 of Algorithm 1. It analyzes the cost of inserting a job j , whose initial task is in position $post_1$ of $S.\sigma^{tasks}$. In line 1, we define $prev$ as the id of the task preceding the task at position $post_1$ in the schedule $S.\sigma^{tasks}$. Next, in line 2 we define st_{t_1} as the start time of the initial task of j , which is right after the conclusion of task $prev$. If the initial task of j overlaps $S.\sigma_{post_1}^{tasks}$ when starting at st_{t_1} (line 3), then we return an infeasible insertion candidate with infinity cost (line 4). In line 5, we calculate st_{t_2} , which is the start time of j 's final task.

The following lines (5-16) of Algorithm 2 will search for the position of j 's final task in $S.\sigma^{tasks}$. Therefore, if j 's final task fits before $S.\sigma_{post_2}^{tasks}$, $post_2 = post_1$ (line 6), when starting at st_{t_2} (line 7), then this insertion candidate is feasible with zero cost. Otherwise, if st_{t_2} is greater than the makespan of S

(line 9), we return a feasible insertion candidate (line 12), whose final task is scheduled at the end of $S.\sigma^{tasks}$ (line 10) with cost $st_{t_2} + b_j - S.C_{max}$ (line 11). If none of the two possibilities holds, it means that j 's final task could only fit in the interval $[post_1 + 1, |S.\sigma^{tasks}|]$. Thus, in line 13, we iteratively search for the expected position h of j 's final task in $S.\sigma^{tasks}$, which is in the interval $[post_1 + 1, |S.\sigma^{tasks}|]$. If j 's final task fits before $S.\sigma_h^{tasks}$ when starting at st_{t_2} (line 14), we return a feasible insertion candidate with zero cost (line 15). Otherwise, the final task overlaps with $S.\sigma_h^{tasks}$. In this case, in line 16, we continue to find a feasible insertion candidate by pushing j while keeping its initial task before $S.\sigma_{post_1}^{tasks}$. Finally, the resulting insertion candidate is returned in line 17.

Algorithm 2: ANALYZE_INSERTION_CANDIDATE($j, post_1, S, I$)

```

1  $prev \leftarrow S.\sigma_{post_1-1}^{tasks};$ 
2  $st_{t_1} \leftarrow S.\tau_{prev} + p_{prev};$ 
3 if  $j$ 's initial task overlaps  $S.\sigma_{post_1}^{tasks}$  when starting at  $st_{t_1}$  then
4   return  $\mathcal{C} : \langle j, \text{false}, post_1, -, st_{t_1}, \infty \rangle;$ 
5  $st_{t_2} \leftarrow st_{t_1} + a_j + L_j;$ 
6  $post_2 \leftarrow post_1;$ 
7 if  $j$ 's final task fits before  $S.\sigma_{post_2}^{tasks}$  when starting at  $st_{t_2}$  then
8   return  $\mathcal{C} : \langle j, \text{true}, post_1, post_2, st_{t_2}, 0 \rangle;$ 
9 if  $st_{t_2} \geq S.C_{max}$  then
10    $post_2 \leftarrow |S.\sigma^{tasks}| + 1;$ 
11    $cost \leftarrow st_{t_2} + b_j - S.C_{max};$ 
12   return  $\mathcal{C} : \langle j, \text{true}, post_1, post_2, st_{t_1}, cost \rangle;$ 
13  $h \leftarrow$  Find the expected position for  $j$ 's final task in the interval  $[post_1 + 1, |S.\sigma^{tasks}|]$ ;
14 if  $j$ 's final task fits before  $S.\sigma_h^{tasks}$  when starting at  $st_{t_2}$  then
15   return  $\mathcal{C} : \langle j, \text{true}, post_1, h, st_{t_1}, 0 \rangle;$ 
16  $\mathcal{C} \leftarrow \text{FIND\_CANDIDATE\_WITH\_PUSH}(j, h, st_{t_1}, st_{t_2}, post_1, S, I);$ 
17 return  $\mathcal{C};$ 

```

Algorithm 3: FIND_CANDIDATE_WITH_PUSH($j, h, st_{t_1}, st_{t_2}, post_1, S, I$)

```

1  $idle \leftarrow$  idle time after  $j$ 's initial task;
2 while  $h < |S.\sigma^{tasks}|$  do
3    $curr \leftarrow S.\sigma_h^{tasks};$ 
4    $push_j \leftarrow S.\tau_{curr} + p_{curr} - st_{t_2};$ 
5   if  $push_j > idle$  then
6     return  $\mathcal{C} : \langle j, \text{false}, post_1, h, st_{t_1}, \infty \rangle;$ 
7   if  $j$ 's final task fits before  $S.\sigma_{h+1}^{tasks}$  when starting at  $st_{t_2} + push_j$  then
8     return  $\mathcal{C} : \langle j, \text{true}, post_1, h + 1, st_{t_1} + push_j, 0 \rangle;$ 
9    $h \leftarrow h + 1;$ 
10   $push_j \leftarrow S.C_{max} - st_{t_2};$ 
11  if  $push_j \leq idle$  then
12    return  $\mathcal{C} : \langle j, \text{true}, post_1, h + 1, st_{t_1} + push_j, p_{2j} \rangle;$ 
13 return  $\mathcal{C} : \langle j, \text{false}, post_1, h, st_{t_1}, \infty \rangle;$ 

```

Algorithm 3 presents the pseudocode for FIND_CANDIDATE_WITH_PUSH, called in line 16 of Algorithm 2. Assuming that j 's final task overlaps task $S.\sigma_h^{tasks}$ when starting at st_{t_2} , it tries to find a feasible insertion candidate for j by pushing its initial and final tasks from their respective start times st_{t_1} and st_{t_2} . Moreover, j 's initial task must still fit before $S.\sigma_{post_1}^{tasks}$. In line 1, we define a variable $idle$ as the idle time after the initial task of j . It indicates the maximum push allowed on j to fit its initial task at $post_1$. In the while loop of lines 2-9, we iteratively analyze whether it is possible to skip the overlapping task $S.\sigma_h^{tasks}$, $h < |S.\sigma^{tasks}|$. In line 3, we store in variable $curr$ the current task $S.\sigma_h^{tasks}$.

After that, in line 4, we calculate $push_j$, which is the necessary push on j for its final task to skip task $curr$. If $push_j > idle$ (line 5), there is no feasible insertion candidate to insert j at pos_{t_1} and we return an infeasible insertion candidate with infinity cost (line 6). Otherwise, the initial task of job j still fits at pos_{t_1} when starting at $st_{t_1} + push_j$. If j 's final task scheduled at $st_{t_2} + push_j$ fits before $S.\sigma_{h+1}^{tasks}$ (line 7), then we return a feasible insertion candidate with zero cost (line 8). In line 9, we iterate the variable h . At the end of the while loop (lines 2-9), $S.\sigma_h^{tasks}$ is the last task of $S.\sigma^{tasks}$. Therefore, we calculate $push_j$ (line 10) and then, if $push_j \leq idle$ (line 11), we return a feasible insertion candidate with cost p_{2j} (line 12). Otherwise, we return an infeasible insertion candidate with infinity cost (line 13).

3.1.3. Time complexity

We argue that our proposed first-fit algorithm is a polynomial-time heuristic with running time in $O(n^3)$, where n is the number of jobs. Note that lines 13 and 16 of Algorithm 2 describe complementary searches, where line 13 loops over $[pos_{t_1}, h]$, and line 16 continues over $[h, |S.\sigma^{tasks}|]$. For that reason, ANALYZE_INSERTION_CANDIDATE has a linear time complexity on the number of jobs, i.e., $O(n)$. In lines 4-11 of Algorithm 1, we run ANALYZE_INSERTION_CANDIDATE for each position after the finish of σ_{i-1}^{jobs} until the end of σ^{tasks} . Thus, the time complexity of lines 4-11 is $O(n^2)$. Additionally, the time complexity of lines 12-16 in Algorithm 1 is $O(n)$, because it applies two linear insertions in the array $S.\sigma^{tasks}$. As the lines 4-17 of Algorithm 1 are executed for each job of σ^{jobs} , the total time complexity of the FIRST_FIT_ALGORITHM is $O(n^3)$.

3.1.4. First-fit quality analysis and alternative strategies

Remember that finding an optimal solution for the SMCTSP is NP-hard even if the sequence for the initial tasks is predefined (Condotta and Shakhlevich, 2012). Accordingly, given the optimal sequence for the initial tasks, our first-fit approach does not guarantee the generation of an optimal solution. We present two instance examples that support the statement, in addition to discussing alternative strategies to generate the optimal schedule for them.

Figure 3 exhibits three schedules for the instance 5_4_L_gen of the benchmark set of Khatami et al. (2019, 2020). (1) **Optimal** is the optimal schedule, which follows the sequence $\sigma^{jobs} = (2, 4, 1, 5, 3)$ for the initial tasks, and the makespan is equal to 490. This same sequence σ^{jobs} passed to our first-fit algorithm yields a different schedule, referred to as (2) **First-fit** in Figure 3, with makespan equal to 629. Despite this difference being significant, our first-fit algorithm can produce several other schedules. Given that the instance 5_4_L_gen contains five jobs, there are $5! = 120$ possible sequences of jobs, meaning that our first-fit algorithm can output 120 different schedules. The best one over them is the schedule (3) **Best first-fit** in Figure 3, which comes from the sequence $\sigma^{jobs} = (1, 2, 4, 3, 5)$. Its makespan is equal to 508, 121 less than the makespan of the schedule (2) **First-fit** in Figure 3, and only 18 ($\approx 3.7\%$) more than the makespan of the schedule (1) **Optimal** in Figure 3.

Observe that, compared to schedule (1) **Optimal** in Figure 3, the schedule (2) **First-fit** in Figure 3 has the same task subsequence before the insertion of $\sigma_5^{jobs} = 3$, i.e., $\sigma^{tasks} = (3, 7, 4, 1, 9, 8, 10, 2)$ is the task subsequence in both schedules disregarding job 3. Our first-fit algorithm does not schedule job 3 before the final task of job 5 because its final task would overlap with the final task of job 1. To accommodate job 3 at its expected position, another strategy is necessary.

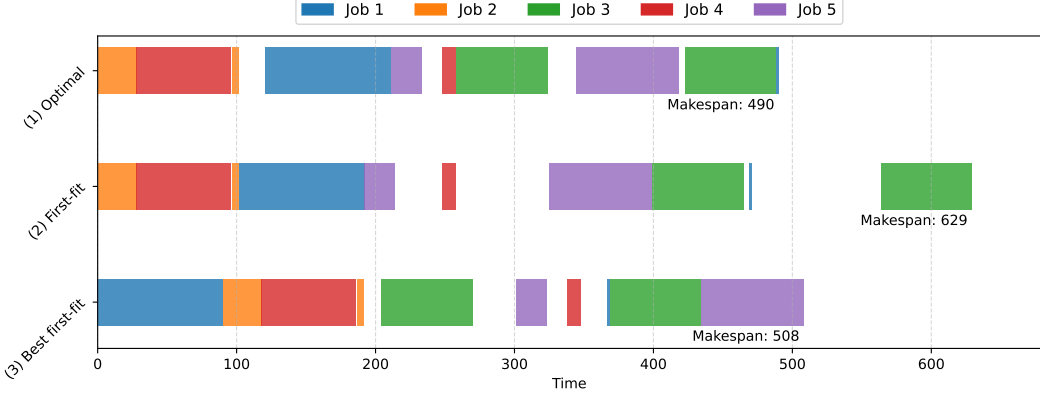


Figure 3: Schedule comparison for instance 5_4_L_gen of the benchmark set of Khatami et al. (2019, 2020).

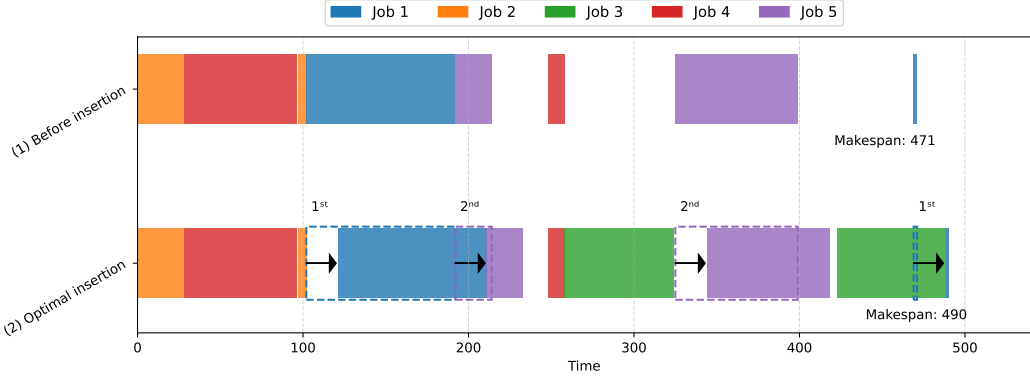


Figure 4: Optimal insertion for instance 5_4_L_gen of the benchmark set of Khatami et al. (2019, 2020). Optimality requires right-shifting jobs 1 and 5.

Figure 4 illustrates a possible strategy to obtain the optimal solution for the instance 5_4_L_gen. Shortly, this strategy modifies our first-fit algorithm to allow right-shifting already scheduled jobs in case of overlaps while maintaining the current task sequence. (1) **Before insertion** is the schedule achieved by our first-fit algorithm before inserting the job 3 in the sequence $\sigma = (2, 4, 1, 5, 3)$, which follows the task subsequence $\sigma^{tasks} = (3, 7, 4, 1, 9, 8, 10, 2)$. (2) **Optimal insertion** displays the optimal schedule and the modifications applied to the schedule (1) **Before insertion** to obtain the optimal insertion for the job 3. An arrow represents the right shift a task received from its previous allocated time, represented by the dashed lines. The ordinal numbers above the arrows denote the sequence of right-shifts on the respective task. Note that, instead of skipping the final task of job 1, we right-shift it to accommodate job 3. Consequently, it would also right-shift the job 5 because the initial task of job 1 would overlap with the initial task of job 5.

Notice that the strategy illustrated in Figure 4 did not modify the sequence σ^{tasks} of the scheduled tasks to accommodate job 3. Even though it is already computationally expensive due to a possible ejection chain, right-shifting scheduled tasks while maintaining the current task sequence to accommodate a job remains a suboptimal approach. Figure 5 illustrates another instance on which the previous strategy would not produce the optimal solution. As for Figure 3, we present three equivalent schedules, but for the instance 5_10_L_gen of the benchmark set of Khatami et al. (2019, 2020).

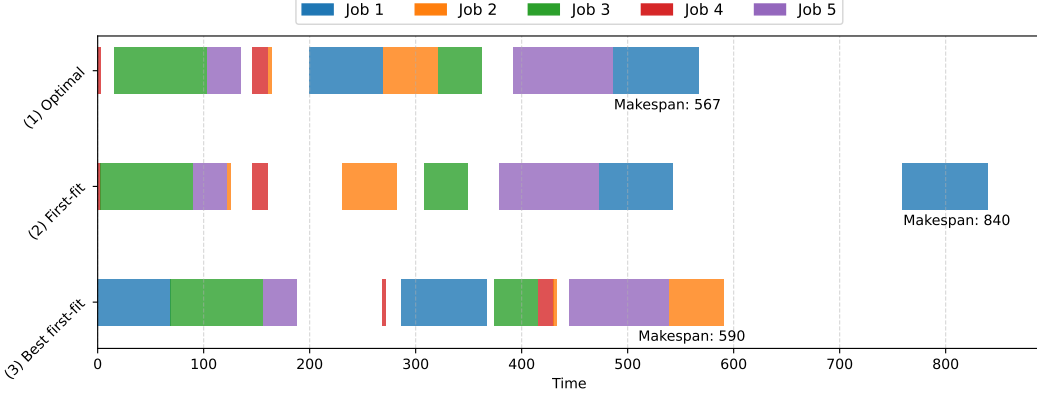


Figure 5: Schedule comparison for instance 5_10_L_gen (Khatami et al., 2019, 2020).

In Figure 5, the schedule (1) **Optimal** follows the sequence $\sigma^{jobs} = (4, 3, 5, 2, 1)$ for the initial tasks, and the makespan equals 567. Similar to Figure 3, this same sequence σ^{jobs} passed to our first-fit algorithm outputs a different schedule, referred to as (2) **First-fit** in Figure 5, with makespan equal to 840. Nevertheless, similarly to instance 5_4_L_gen, our first-fit algorithm can output 120 different schedules for instance 5_10_L_gen. The best one over them is the schedule (3) **Best first-fit** in Figure 5, which comes from the sequence $\sigma^{jobs} = (1, 3, 5, 4, 2)$. Its makespan is equal to 590, 250 less than the makespan of the schedule (2) **First-fit**, and only 23 ($\approx 4.1\%$) more than the makespan of the schedule (1) **Optimal**.

Notice that, disregarding job 1, the task subsequence of the schedule (1) **Optimal** in Figure 5 is $\bar{\sigma}^{tasks} = (7, 5, 9, 8, 3, 4, 6, 10)$, while the task subsequence of the schedule (2) **First-fit** in Figure 5 is $\bar{\sigma}^{tasks} = (7, 5, 9, 3, 8, 4, 6, 10)$. Remark that the initial task of job 2 (task 3) is placed at position 5 in schedule (1) **Optimal**, while this same task is placed at position 4 in schedule (2) **First-fit**. This suggests another strategy different from the one depicted in Figure 4.

Figure 6 shows another strategy to obtain the optimal solution for the instance 5_10_L_gen. Similar to Figure 4, the arrows, dashed lines, and the ordinal numbers above the arrows detail the strategy, which allows modifications on the task sequence $\bar{\sigma}^{tasks}$. In this scenario, the first four jobs of σ^{jobs} would be inserted the same way as our first-fit algorithm. For the fifth job ($\sigma_5^{jobs} = 1$), however, the new strategy would move the initial task of job 2 to position 5 after a series of right-shifts. We don't analyze the step-by-step process to insert job 1, although the reader might come up with the same solution based on the arrows, dashed lines, and the ordinal numbers denoting the sequence of the right-shifts. Jobs with two ordinal numbers mean that they were right-shifted twice.

Even though the two presented strategies may yield optimal schedules for a larger set of instances, their computational complexity is significantly greater than our first-fit algorithm. Furthermore, this trade-off might not be worth it in practice when using them in BRKGA's decoder. The presented examples show that the best first-fit schedules are reasonably good approximations to the optimal schedules, and the BRKGA embedded with such a decoder will be able to explore the set of possible solutions more efficiently.

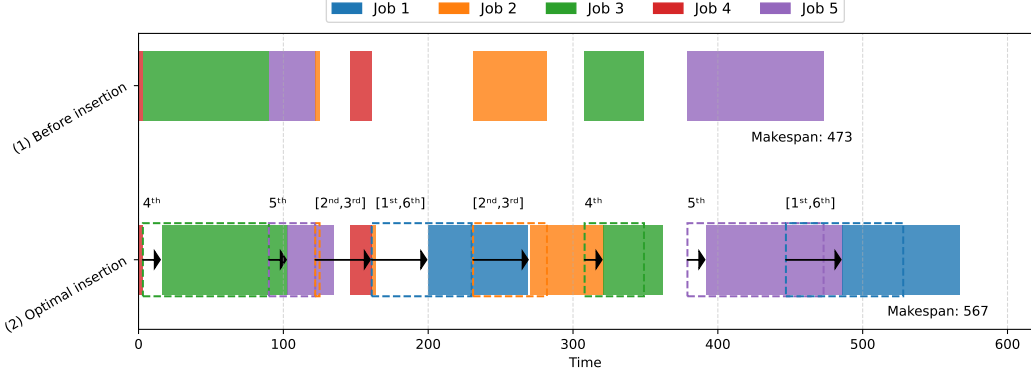


Figure 6: Optimal insertion for instance 5_10_L_gen of the benchmark set of Khatami et al. (2019, 2020). Optimality requires right-shifting jobs 1, 2, 3, and 5. The initial task of job 2 skips the final task of job 4.

3.2. Initial solution generator

In a standard BRKGA, the initial population contains only random individuals. Londe et al. (2025) cited several authors who show the benefits of providing good solutions as individuals in the initial population. In this work, we set part of the initial population with the best solutions of a multi-start procedure. We first execute an adaptive version of the decoder, described in Algorithm 4. Thereafter, we perform multiple executions of its randomized version, described in Algorithm 5. The best $m \leq p$ solutions are converted into individuals of the initial population. The remaining $p - m$ individuals are generated randomly as standard. Preliminary experiments showed that passing a percentage of the multi-start solutions can be beneficial. Thus, we set $m = \lambda^{ws} \cdot p$, where λ^{ws} is an input parameter defining the percentage of the initial population filled with the best multi-start solutions.

Algorithm 4 describes the pseudocode for the FIRST_FIT_ADAPTIVE called in the multi-start procedure. Lines 1-2 start the partial solution S by inserting the job with the longest delay at the beginning of the schedule. Lines 3-4 keep track of the last job inserted in S and create a set R of the remaining jobs to be inserted, i.e., not yet in the solution. After that, the for loop of lines 5-13 schedules the remaining jobs in R . Line 6 initializes the best insertion candidate BC with infinity cost to serve as a sentinel, as this is a minimization problem. Next, the for loop of lines 7-10 looks for the least cost first-fit insertion candidate among all remaining jobs $j \in R$. As in lines 5-11 of Algorithm 1, we also execute ANALYZE_INSERTION_CANDIDATE(j, pos_1, S, I) (Algorithm 2) in line 8 of Algorithm 4 for every position pos_1 after the $last_{job}$'s initial task in schedule $S.\sigma^{tasks}$ to insert job j . In lines 9 and 10, BC is updated every time $C.cost < BC.cost$. At the end of the for loop of lines 7-10, we update the partial solution S as in lines 12-16 of Algorithm 1, i.e., by inserting $BC.j$ according to BC (line 11). Subsequently, we update $last_{job}$ (line 12) and remove it from the remaining jobs R . Finally, after the for loop of lines 5-13, S contains a feasible schedule for all jobs $j \in J$ and we return S (line 14).

Algorithm 4: FIRST_FIT_ADAPTIVE(I)

```

1  $j \leftarrow$  job with the longest delay;
2  $S \leftarrow$  Partial solution with the  $j$  scheduled at time 0;
3  $last_{job} \leftarrow j$ ;
4  $R \leftarrow$  Copy of  $J \setminus \{last_{job}\}$ ;
5 for  $i \leftarrow 2$  to  $n$  do
6    $BC \leftarrow \mathcal{C} : \langle 0, \text{false}, 0, 0, 0, \infty \rangle$ ;
7   for  $j \in R$  do
8      $\mathcal{C} \leftarrow$  First-fit insertion candidate after  $last_{job}$ 's initial task in  $S.\sigma^{tasks}$  to insert  $j$ ;
9     if  $\mathcal{C}.cost < BC.cost$  then
10        $BC \leftarrow \mathcal{C}$ ;
11    $S \leftarrow$  Update partial solution  $S$  by inserting  $BC.j$  according to  $BC$ ;
12    $last_{job} \leftarrow BC.j$ ;
13   Remove  $last_{job}$  from  $R$ ;
14 return  $S$ ;

```

Algorithm 5 describes the randomized version of the FIRST_FIT_ADAPTIVE presented in Algorithm 4. The main differences are highlighted in the following. First, in line 1, the first job of the schedule is selected randomly. Then, we initialize an empty insertion candidate list (line 6). It will store all the first-fit insertion candidates \mathcal{C} of the jobs $j \in R$ (line 9). Afterward, an insertion candidate is chosen from CL by randomly selecting an insertion candidate \mathcal{C} from CL restricted by quality, which requires a threshold parameter $\alpha \in [0, 1]$. For this, in line 10, we create a restricted insertion candidate list RCL composed of insertion candidates $\mathcal{C} \in CL$, whose cost $\mathcal{C}.cost$ lies in the interval $[c_{min}, c_{min} + \alpha(c_{max} - c_{min})]$, where $c_{min} = \min(\mathcal{C}.cost : \mathcal{C} \in CL)$, and $c_{max} = \max(\mathcal{C}.cost : \mathcal{C} \in CL)$. Later, in line 11, we randomly choose an insertion candidate \mathcal{C} from RCL . Note that for $\alpha = 0$, the FIRST_FIT_ADAPTIVE_RANDOMIZED is not equivalent to the FIRST_FIT_ADAPTIVE of Algorithm 4 because two insertion candidates in RCL can have the same cost, i.e., the algorithm can randomly choose between them, instead of selecting the first one found.

Algorithm 5: FIRST_FIT_ADAPTIVE_RANDOMIZED(I, α)

```

1  $j \leftarrow$  random job;
2  $S \leftarrow$  Partial solution with the  $j$  scheduled at time 0;
3  $last_{job} \leftarrow j$ ;
4  $R \leftarrow$  Copy of  $J \setminus \{last_{job}\}$ ;
5 for  $i \leftarrow 2$  to  $n$  do
6    $CL \leftarrow \emptyset$ ;
7   for  $j \in R$  do
8      $\mathcal{C} \leftarrow$  First-fit insertion candidate after  $last_{job}$ 's initial task in  $S.\sigma^{tasks}$  to insert  $j$ ;
9     Add  $\mathcal{C}$  to  $CL$ ;
10   $RCL \leftarrow CL$  filtered by quality using threshold parameter  $\alpha$ ;
11   $\mathcal{C} \leftarrow$  Random candidate from  $RCL$ ;
12   $S \leftarrow$  Update partial solution  $S$  by inserting  $\mathcal{C}.j$  according to  $\mathcal{C}$ ;
13   $last_{job} \leftarrow \mathcal{C}.j$ ;
14  Remove  $last_{job}$  from  $R$ ;
15 return  $S$ ;

```

3.3. Local search

Londe et al. (2025) presented an extensive list of authors that applied local search (LS) algorithms in the BRKGA. They hybridize the LS with the BRKGA in several ways. In this work, we combine two of these ideas. First, inspired by Andrade et al. (2019), we periodically apply the local search to the best individual of the elite set. Second, inspired by Silva et al. (2025), we apply the local search after an improvement on the best b individuals of the elite set. Besides, our LS method is a modification of the commonly used *insert* method (den Besten and Stützle, 2001). Our modification allows more control

over the neighborhood size. In this paper, we adopted the term *move* instead of *insert* for this method. In what follows, we describe our neighborhood structure design (Section 3.3.1), present the local search algorithm (Section 3.3.2), and detail the integration with the BRKGA (Section 3.3.3).

3.3.1. Local search neighborhood

Remember that in Section 3.1 we stated that our first-fit algorithm is injective. Thus, we represent each solution by the sequence σ^{jobs} retrieved from a vector of random keys X . Given a sorted sequence of the jobs σ^{jobs} of an individual of the current BRKGA population, define the *move* operation as one that removes the job in position i and inserts it in position j of σ^{jobs} . A neighbor of σ^{jobs} is a sorted sequence that can be obtained from σ^{jobs} through a *move* operation. The size of this neighborhood is known to be $(n - 1)^2$ (den Besten and Stützle, 2001).

Notice that the makespan calculus of each neighbor could lead to an ejection chain that reconstructs the entire solution. This ejection chain is mainly caused by interleaving jobs, i.e., when tasks of different jobs are scheduled between a job's tasks. Therefore, we run the FIRST_FIT_ALGORITHM described in Algorithm 1, which has a time complexity of $O(n^3)$ (see Section 3.1.3). Consequently, the time complexity of one LS iteration is $O(n^5)$. Given that we execute the LS periodically, this method becomes computationally expensive. On that account, we propose a parameter that controls the neighborhood size. Given a sorted sequence σ^{jobs} , define the radius r as the extension of the *move* operation, i.e., σ_k^{jobs} ($1 \leq k \leq n$) can only be moved to position l ($\max(1, k - r) \leq l \leq \min(k + r, n)$). Figure 7 illustrates the *move* candidates of a job within a radius and the result of a *move* operation.

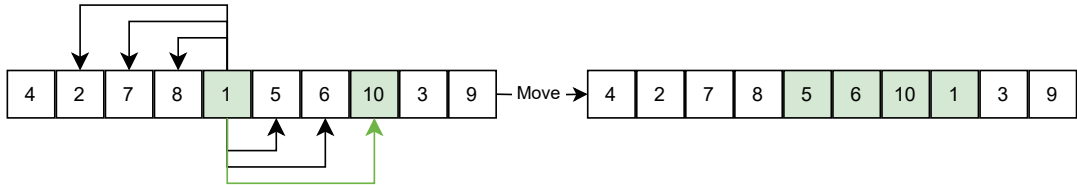


Figure 7: Move candidates for $\sigma_5^{jobs} = 1$ with radius $r = 3$ and a move operation.

Given that we apply the LS in two different situations, we denote by r_{pLS} and r_{iLS} the radius values for the periodic LS and the LS after an improvement, respectively. Note that, if the radius r of the LS iteration is bounded above by a small constant, the number of neighbors becomes $O(n)$, which also decreases the time complexity of one LS iteration from $O(n^5)$ to $O(n^4)$.

3.3.2. Local search algorithm

Algorithm 6 describes the local search algorithm, which receives as input a random-key vector X , its makespan C_{max} , the local search radius r and the instance I . In lines 1-2, we initialize the best random-key vector and its makespan. Next, we first set a flag *impr* as **true** (line 3) to enter the while loop (line 4), then we set it to **false** (line 5). If an improving neighbor is found during the while loop of lines 4-22, *impr* becomes **true** and we initiate a new LS iteration (line 4). Otherwise, we leave the while loop because we reached a local optimum. In line 6, we generate the sorted sequence σ^{jobs} of the

random-key vector X^* (see Section 3.1). In line 7, we set a new variable k as 1, referencing the job σ_k^{jobs} to be moved.

Afterward, in the while loop of the lines 8-22, we analyze, for each $k \in \{1, \dots, n\}$, each move candidate of the job σ_k^{jobs} (see Figure 7) until an improvement is found (i.e., $impr = \text{true}$) or all jobs have been analyzed (i.e., $k > n$). In line 9, we initialize variable l as $\max(1, k - r)$, which stores the destination candidate of the job σ_k^{jobs} . In line 10, we move the job σ_k^{jobs} to position l in σ^{jobs} to start the analysis of the move candidates.

In the while loop of the lines 11-18, we increment over the extension of the move operation (i.e., $l \leq k + r$) until we reach the end of the schedule (i.e., $l \leq n$) or find an improvement (i.e., $impr = \text{true}$). In line 12, we check whether the candidate move destination is valid by ensuring it is neither the origin (i.e., $l \neq k$) nor a previously analyzed neighbor (i.e., $l \neq k - 1$). Consequently, when this condition is met, line 13 decodes σ^{jobs} to yield the corresponding solution S . If the makespan of S is smaller than the makespan of X^* (line 14), an improvement was found. Therefore, in line 15, we update the best makespan C_{max}^* , the best random-key vector X^* , and activate the flag $impr$. Then, if the next job destination is within the schedule (line 16), we swap σ_l^{jobs} with σ_{l+1}^{jobs} (line 17), i.e., the moving job that was in position l is now placed in position $l + 1$. Next, we increment l (line 18).

At the end of the while loop of lines 11-18, there are two possible outcomes. First, all move candidates were analyzed, and no improvement was found. In this case (line 19), we return the moving job that is in position $\min(l, n)$ (line 20) to its original position k in σ^{jobs} (line 21) and we increment k to analyze the next move candidates for job σ_{k+1}^{jobs} (line 22). Otherwise, an improvement was found and σ^{jobs} is the improving neighbor. Therefore, we leave the loop of lines 11-22 and start a new local search round. After the loop of lines 4-22, X^* encodes a local optimum solution and C_{max}^* corresponds to its makespan. Thus, in line 23, we return both variables.

Algorithm 6: MOVE_JOB_FIRST_IMPROVEMENT(X, C_{max}, r, I)

```

1  $X^* \leftarrow \text{copy of } X;$ 
2  $C_{max}^* \leftarrow C_{max};$ 
3  $impr \leftarrow \text{true};$ 
4 while  $impr$  do
5    $impr \leftarrow \text{false};$ 
6    $\sigma^{jobs} \leftarrow \text{sorted sequence of the jobs of the vector } X^*;$ 
7    $k \leftarrow 1;$ 
8   while  $k \leq n$  and not  $impr$  do
9      $l \leftarrow \max(1, k - r);$ 
10     $\sigma^{jobs} \leftarrow \text{Move } \sigma_k^{jobs} \text{ to position } l \text{ in } \sigma^{jobs};$ 
11    while  $l \leq \min(k + r, n)$  and not  $impr$  do
12      if  $l \neq k$  and  $l \neq k - 1$  then
13         $S \leftarrow \text{FIRST\_FIT\_ALGORITHM}(\sigma^{jobs}, I);$ 
14        if  $S.C_{max} < C_{max}^*$  then
15           $\left[ \begin{array}{l} \text{Update } C_{max}^*, X^* \text{ and set } impr \leftarrow \text{true}; \\ \dots \end{array} \right]$ 
16        if  $l + 1 \leq n$  then
17           $\left[ \begin{array}{l} \sigma^{jobs} \leftarrow \text{Swap } \sigma_l^{jobs} \text{ with } \sigma_{l+1}^{jobs}; \\ \dots \end{array} \right]$ 
18         $l \leftarrow l + 1;$ 
19      if not  $impr$  then
20         $l \leftarrow \min(l, n);$ 
21         $\sigma^{jobs} \leftarrow \text{Move } \sigma_l^{jobs} \text{ to position } k \text{ in } \sigma^{jobs};$ 
22         $k \leftarrow k + 1;$ 
23 return  $X^*, C_{max}^*$ 

```

3.3.3. Integration with the BRKGA

We propose to execute the LS in two situations: (i) periodically and (ii) after an improvement. The periodic LS is set to run every L iterations on the best eligible individual of the current elite set. After each periodic LS, we mark the individual as ineligible for another periodic LS. We also set L to be proportional to the number of jobs n . The LS after an improvement occurs on the best b eligible individuals of the elite set. Similar to the periodic LS, we mark each individual as ineligible for any other LS. Note that, for $r_{pLS} < r_{iLS}$, the LS after an improvement can still be executed on the individual that has already undergone a periodic LS. In turn, the periodic LS is not applied to the individual on whom the LS was performed after an improvement. Besides, given a population P sorted by fitness, whenever we search for the next best individual, we store the fitness of the previously analyzed individual $i \in P$. If the next individual $i + 1 \in P$ has the same fitness, we skip the LS execution.

Table 2 illustrates an example of LS eligibility within the elite set. Column “Pos.” shows each individual’s position. Column “Eligibility” lists four cases: “Ineligible (I)” when LS was applied after an improvement; “Ineligible (P)” when a periodic LS was applied; “Eligible” when no LS was applied; and “Same fitness” when its fitness matches that of someone ranked above. Finally, column “Fitness” exhibits the fitness of the individual. Assuming $b = 2$, observe that the LS after an improvement would be executed on the second and third individuals of the elite set, while the periodic LS would be executed only on the fourth individual.

Table 2: Example of LS eligibility within the elite set

Pos.	Eligibility	Fitness
1	Ineligible (I)	4347
2	Ineligible (P)	4524
3	Ineligible (P)	4554
4	Eligible	4562
5	Ineligible (P)	4599
6	Eligible	4845
7	Same fitness	4845
8	Eligible	4846
9	Eligible	4860
10	Eligible	4862

3.4. Perturbation

This section describes the perturbation component of our BRKGA. Throughout the generations, the BRKGA aims to improve the population by combining pairs of solutions from the elite and non-elite sets, but biased towards the elite solutions. After a certain number of iterations, the BRKGA expects the elite set to contain a set of blocks of keys in the random-key vectors that positively impact the quality of a solution. We denote this set as the *convergence structure*. Notwithstanding this, the BRKGA may eventually reach many generations without improving the overall best solution. The metaheuristics generally contain a diversification mechanism to overcome this situation, which can provide new search directions. For the BRKGA, it consists of the insertion of randomly generated individuals. However, sometimes this may not be sufficient to produce improved solutions, and adding a perturbation component such as a restart can be beneficial.

During some preliminary tests, we noticed that parameter configurations can highly affect the number of unique random-key vectors in a population throughout the generations. In Appendix B, we show the correlation between the percentage of unique random-key vectors in a population and (i) the elite percentage p_e , (ii) the mutant percentage p_m , (iii) and the inheritance probability of an elite parent key ρ_e . In summary, BRKGA-R can quickly converge to a homogeneous elite set after each restart. Additionally, for higher p_e , lower p_m , and higher ρ_e , part of the non-elite set becomes less diverse. This is a common concern in genetic algorithms, denoted as *premature convergence* (Fogel, 1994), and there are some approaches to prevent it in genetic algorithms (Pandey et al., 2014). Londe et al. (2024) states that in a BRKGA, the premature convergence is related to a lack of diversity in the elite set, although we also observed it in the non-elite set. They also review some operators to prevent the premature convergence, including the island model (Pandey et al., 2014; Whitley et al., 1999), the reset operator, and the shake (Andrade et al., 2019).

Given that we observed this issue even with the restarts, a possible workaround would be to reduce the restart periodicity. The problem with this approach is that each time a population is restarted, it destroys the convergence structure of the population, i.e., valuable parts of the random-key vector that usually appear in better solutions can be lost. On that account, we adopted the *shaking* method, a BRKGA feature introduced by Andrade et al. (2019) to deal with this scenario. It randomly modifies the individuals in the elite set and restarts only the non-elite set, instead of restarting the whole population. Hence, the elite set will preserve some parts of the convergence structure.

3.4.1. Shaking

The original BRKGA shaking method proposed by Andrade et al. (2019) is executed over the problem solution space, i.e., over the decoded solutions. Some authors followed this approach (Londe et al., 2021; Kim and Lee, 2024). On the other hand, other authors have proposed to shake over the BRKGA space, i.e., over the random-key vectors (Londe et al., 2022; Mauri et al., 2021). In this work, we employ the shaking method implemented in the framework of Andrade et al. (2021), which performs the operations over the BRKGA space. In summary, the shaking method performs $\psi = \lambda^{shake} \cdot n$ pairs of random operations in each elite set individual and replaces the non-elite set members with random samples. The parameter $\lambda^{shake} \in [0, 1]$ is a percentage of the number of jobs. There are two types of shaking (s^{type}): *CHANGE* and *SWAP*. In *CHANGE*, it first selects a random key and inverts its value. Then, it selects another random key and replaces its value with another random value. In *SWAP*, it first selects a random key and swaps its value with the following key's value. In sequence, it selects two random keys and swaps their values.

As the *shaking* method enables more frequent perturbations, it can be applied in more situations. To address the issue of premature convergence, we apply a weak shake each time the elite set becomes homogeneous, i.e., the best fitness is equal to the worst fitness of the elite set. We define the weak shake as Andrade et al. (2019), i.e., λ^{shake} is uniformly drawn from the interval $[0.05, 0.2]$. Sometimes, the BRKGA gets stuck, and the weak shake may not help the BRKGA to find new improved solutions. In this case, we first define z as the current number of iterations without improvement. Then, we apply a strong shake each time $z \bmod R^{**} = R$, where R^{**} defines the length of the perturbation cycle and R defines the strong shake iteration in this perturbation cycle. We define the strong shake as Andrade et al.

(2019), i.e., λ^{shake} is uniformly drawn from the interval $[0.5, 1.0]$. Finally, we still reset the population each time $z \bmod R^{**} = R^*$, $R^* > R$, where R^* defines the restart iteration in the perturbation cycle. Figure 8 illustrates the perturbation cycle of our BRKGA.

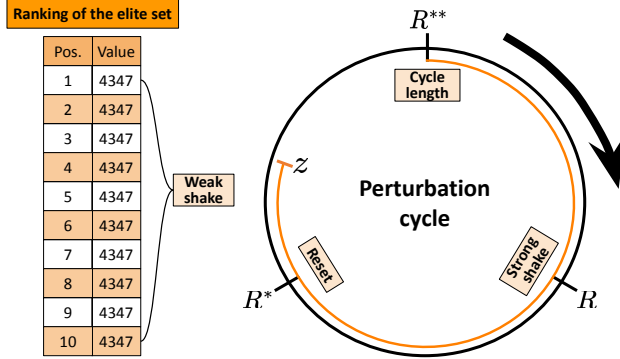


Figure 8: Perturbation cycle of our BRKGA

However, some observations indicated that the BRKGA may lose its convergence structure even when we apply a weak shake. This is similar to what happens when resetting the population. Some authors solve this issue by injecting a random-key vector, such as the overall best solution found so far or the best initial solution (Festa et al., 2024; de Abreu et al., 2022; Andrade et al., 2019), but this has not been applied after the *shaking* to our knowledge. Nonetheless, preliminary tests showed that injecting a random-key vector can be beneficial. Accordingly, we selected some injection candidates from the preliminary tests. The first candidate is the type “best solution of the current population”, denoted as CB. It is a good candidate to inject after a weak shake, as we want to preserve the convergence structure. The second candidate is the type “best overall solution found so far”, denoted as OB. It performs well after each type of perturbation, whether it is a weak shake, a strong shake, or a population reset. The third candidate is the type “best solution of a new multi-start execution”, denoted as BMS. Instead of injecting the initial solution again, we provide a new random solution with potentially new and useful parts. We define parameters that indicate the type of solution to be injected after a weak shake (γ^{weak}), a strong shake (γ^{strong}), and a reset (γ^{reset}), where $\gamma^{weak} \in \{CB, OB\}$, $\gamma^{strong} \in \{OB, BMS\}$, and $\gamma^{reset} \in \{OB, BMS\}$. Figure 9 displays the injection strategy after perturbations in our BRKGA.

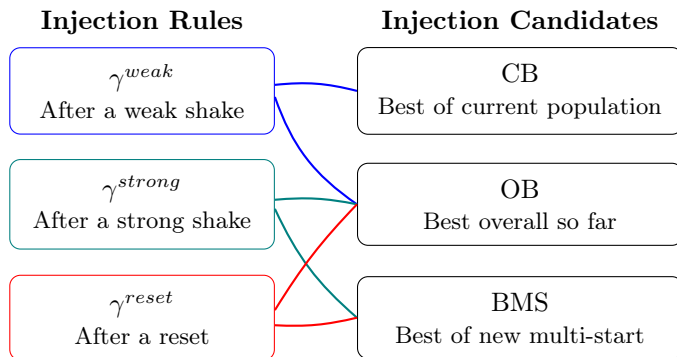


Figure 9: Injection strategy after perturbations in our BRKGA.

3.5. Overall framework

Figure 10 depicts our proposed BRKGA’s flowchart for the single-machine CTSP. The baseline BRKGA-R is presented in blue, while the additional components of the BRKGA-R-S-LS are highlighted in green. In the beginning, we generate $\lceil \lambda^{ws} \cdot p \rceil$ solutions with the initial solution generator (see Section 3.2), where p is the population size, and λ^{ws} is the percentage of these solutions that will be inserted into the initial population. Then, we encode these solutions and generate other $\lfloor (1 - \lambda^{ws}) \cdot p \rfloor$ random-key vectors to construct the initial population. The random-key vectors of the initial population are decoded and sorted by their fitness. Afterward, the main loop of the BRKGA starts. At the beginning of each BRKGA iteration, we compute the next generation of the population based on solution quality. Consequently, we classify the solutions as elite or non-elite, where the first $\lfloor p_e \cdot p \rfloor$ solutions compose the elite set. Then, the next population consists of: the current elite set, a set of $\lfloor p_m \cdot p \rfloor$ mutant solutions, and the remaining solutions resulting from the combination of elite and non-elite solutions. Afterward, the non-decoded random-key vectors are decoded and sorted by their fitness. Given an iteration i of the main BRKGA loop, we execute the periodic LS on the best eligible individual of the population whenever $i \bmod L = 0$ (see Section 3.3.3). If an overall improvement was found in the current generation, we apply the LS on the best b eligible individuals and update the best overall individual (see Section 3.3.3). After that, we consider three perturbations (see Section 3.4). First, if the condition for a weak shake is satisfied, we apply it and inject the solution of type γ^{weak} . Second, if the condition for a strong shake is satisfied, we apply it and inject the solution of type γ^{strong} . Third, if the condition for a restart is satisfied, we restart the BRKGA, resetting the population by replacing it with $p - 1$ new random-key vectors and the solution of type γ^{reset} . While the stopping rule is not satisfied, we repeat the process. Otherwise, the algorithm finishes, and the best random-key vector obtained is returned.

4. Computational experiments

In this section, we present the computational results to evaluate the performance of the CP model and the BRKGA metaheuristic approaches. All experiments were conducted on a machine running Ubuntu x86-64 GNU/Linux, with an Intel Core i7-10700 Octa-Core 2.90 GHz processor and 16 GB of RAM. The CP model was implemented in MiniZinc version 2.8.7 (Nethercote et al., 2007; Stuckey et al., 2014) and solved with OR Tools CP-SAT version 9.11.4210 (Perron and Didier, 2024). It is worth highlighting that we use the MiniZinc’s predicate `disjunctive` for the noOverlap global constraint (3) in the CP model (see Section 2). The BRKGA was implemented in Julia version 1.11.3, based on the BrkgaMpIpr.jl framework (Andrade, 2019; Andrade et al., 2021). We also implemented the state-of-the-art MIP formulations of Khatami and Salehipour (2024) in Julia 1.11.3, using the following packages: JuMP v1.23.6, Gurobi v1.5.0, Gurobi_jll v12.0.2.

We organize this section as follows. Section 4.1 presents the benchmark instances. Section 4.2 lists the tested approaches and details the parameter settings. Section 4.3 compares the CP with the state-of-the-art MIP formulations. Section 4.4 shows a comparison between our approaches and the best-known solutions. Section 4.5 compares the tested approaches with each other under the same computational settings. Section 4.6 analyzes the impact of the BRKGA components.

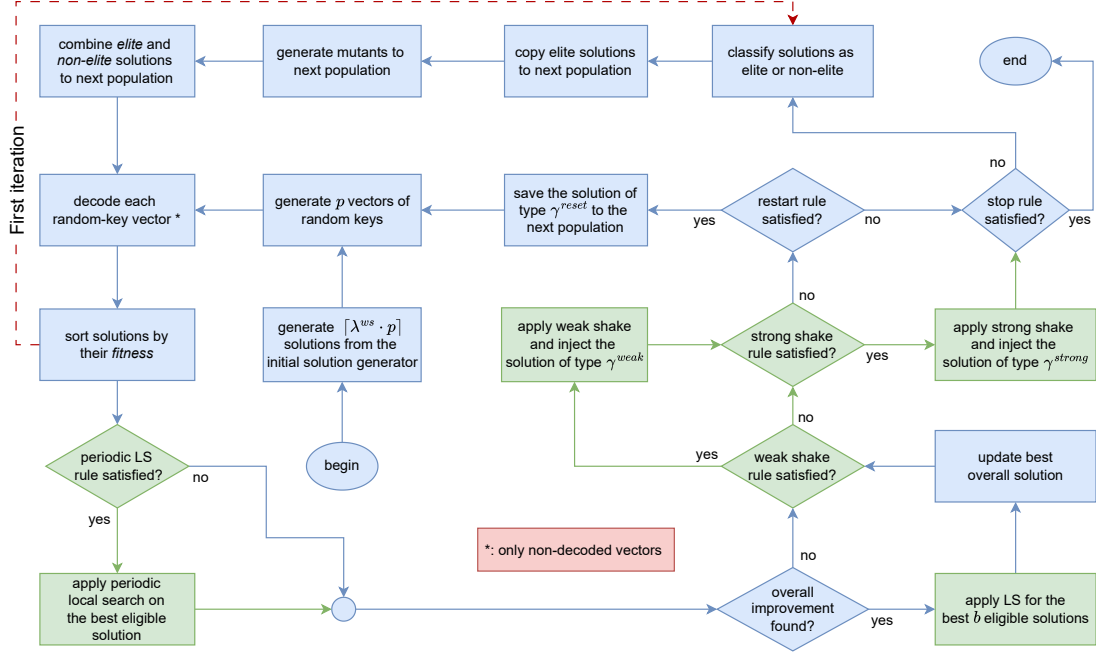


Figure 10: Flowchart of the BRKGA approaches used in this paper for the single-machine CTSP. In blue, the baseline BRKGA-R. In green, the BRKGA-R-S-LS.

4.1. Benchmark instances

We considered the general benchmark set proposed in Khatami et al. (2019, 2020). There are eight different numbers of jobs, i.e., $n \in \{5, 10, 15, 20, 25, 40, 50, 100\}$. For each value of n , there are 30 randomly generated instances divided into three categories: small (S), medium (M), and large (L). In total, there are 240 instances. Each category has 10 instances, where the processing time of the tasks and the delay durations are drawn from the discrete uniform distribution with the following parameters: for category S, $a_j, b_j \sim U(1, 20)$ and $L_j \sim U(10, 80)$; for category M, $a_j, b_j \sim U(1, 50)$ and $L_j \sim U(25, 200)$; and for category L, $a_j, b_j \sim U(1, 100)$ and $L_j \sim U(50, 400)$. The instances are represented as $n_id_category_gen$, where $id \in [1, 10]$ and “gen” indicates that the instances are part of the general set proposed by Khatami et al. (2020).

4.2. Tested approaches and parameter settings

The following approaches were evaluated in the computational experiments:

- the CP model described in Section 2, denoted as CP;
- the BRKGA with the restart presented in Section 3, denoted as BRKGA-R;
- the BRKGA with the restart, the shake, and the local search detailed in Section 3, denoted as BRKGA-R-S-LS;
- the MIP formulation of Békési et al. (2014), denoted as MIP_P1 (Khatami and Salehipour, 2024);
- the MIP formulation of Khatami and Salehipour (2024), denoted as MIP_P2.

We execute ten independent runs of each BRKGA metaheuristic in a single thread for three minutes. We remark that we don't compare the BRKGAs with the state-of-the-art heuristics of [Khatami and Salehipour \(2024\)](#) (BS_P1, BS_P2, and R&S) since they are based on mathematical formulations and require significantly more time (60 minutes) to obtain competitive results compared to our BRKGAs, which are designed to run within low computational times (three minutes in our tests). We run the OR Tools CP-SAT with two different setups. The first executes one run in a single thread with a time limit of three minutes, only to compare with the BRKGA metaheuristics. The second uses eight threads with a time limit of one hour to: (1) find optimal solutions; (2) compute the best objective values and lower bounds; and (3) compare with the state-of-the-art MIP formulations. Both setups stop when they find an optimal solution, or they reach their respective time limits. In terms of notation, we additionally add a suffix to differentiate the setups. CP-1T denotes the CP executed with one thread and a time limit of three minutes, while CP-8T denotes the CP executed with eight threads and a time limit of one hour. For the state-of-the-art formulations MIP_P1 and MIP_P2, we execute one run of the solver using eight threads with a time limit of one hour to compare with the CP-8T.

We have many parameters to set up for the two BRKGA approaches we implemented (see Section 3). Therefore, we employed the `irace` package version 4.2.0 developed by [López-Ibáñez et al. \(2016\)](#) to define the parameters for each algorithm. Table 3 presents the parameter settings suggested by `irace`. We assume $r_{iLS} = n$, i.e., we search the whole neighborhood for the LS after an improvement. Besides, we also assume $\gamma^{reset} \in \{\text{OB, BI, BMS}\}$ for the BRKGA-R, where BI is the type “best initial solution”. It is worth mentioning that setting $\gamma^{reset} = \text{CB}$ is equivalent to assuming $\gamma^{reset} = \text{OB}$ for the BRKGA-R. For details on the parameters and configurations, see Appendix A.

Table 3: Summary of the parameters, their definitions, and the settings suggested by `irace`

Component	Notation	Definition	BRKGA-R		BRKGA-R-S-LS	
			Used	<code>irace</code>	Used	<code>irace</code>
Standard	n	number of random keys in a solution	✓	—	✓	—
	p	population size	✓	163	✓	185
	p_e	elite population size	✓	0.39	✓	0.43
	p_m	mutant population size	✓	0.20	✓	0.24
	ρ_e	probability of inheritance of an elite parent key	✓	0.74	✓	0.78
Initial solution generator	α	threshold parameter for quality selection	✓	0.02	✓	0.01
	λ^{ws}	percentage of the initial population from multi-start	✓	0.28	✓	0.22
	n_{msi}	number of multi-start iterations	✓	1374	✓	602
Perturbation	n_{nimp}	restart cycle while no improvement	✓	956	—	—
	R	strong shake iteration in the perturbation cycle	—	—	✓	154
	R^*	restart iteration in the perturbation cycle	—	—	✓	$2 \cdot R$
	R^{**}	length of the perturbation cycle	—	—	✓	$9 \cdot R$
	s^{type}	shake type — {CHANGE, SWAP}	—	—	✓	SWAP
	γ^{weak}	type of solution injected after a weak shake	—	—	✓	OB
	γ^{strong}	type of solution injected after a strong shake	—	—	✓	OB
	γ^{reset}	type of solution injected after a reset	✓	BMS	✓	OB
Local search	b	max. number of elite-set individuals for LS after improvement	—	—	✓	9
	L	LS periodicity	—	—	✓	$0.21 \cdot n$
	r_{pLS}	LS radius for periodic LS	—	—	✓	7
	r_{iLS}	LS radius for LS after improvement	—	—	✓	—

4.3. Comparison between the CP and the state-of-the-art MIP formulations

In this section, we compare the CP-8T against the MIP_P1 and MIP_P2 of [Khatami and Salehipour \(2024\)](#) within the same computational environment (see Section 4.2). The MIP approaches obtained feasible solutions for 230 (MIP_P1) and 206 (MIP_P2) out of the 240 instances (95.83% and 85.83%). We highlight that MIP_P2 did not obtain a feasible solution for any instance with 100 jobs. Nonetheless, our CP-8T obtained feasible solutions for all instances. Besides, the CP-8T and the MIP approaches achieved optimal solutions for every instance with up to ten jobs in at most 30 seconds. Since no further improvements are possible for these instances with up to ten jobs, we disregard their results. Additionally, we omit the execution time of the three approaches because almost all of them reached 3600 seconds for the considered instances (except some instances with 15 jobs).

Table 4 presents an overview of the CP-8T results compared to the MIP_P2 and MIP_P1 for $n \geq 15$, grouped by their number of jobs n and their category cat . We denote each group as $\langle n \rangle \times \langle \text{cat} \rangle$, where $\langle n \rangle$ is the number of jobs and $\langle \text{cat} \rangle$ is the category of the instances. We consider the following metrics over each group: the mean objective value, the mean optimality gap (in percentage), and the number of optimal solutions. The optimality gap is calculated as: $100 \cdot \frac{|\text{value} - \text{bound}|}{\text{value}}$, where bound is the objective bound, and value is the objective value. The value “NA” (Not Applicable) is placed whenever the solver on the respective formulation did not find a feasible solution for at least one instance of the group. The row **Total** summarizes the results of all the instances by summing the columns. The row **Mean** summarizes the results of all the instances by taking the mean of the columns, but only for the applicable rows without “NA” in the three formulations.

Table 4: Overview of the CP-8T results compared to the MIP_P1 and MIP_P2

n	cat	Objective value			Optimality gap (%)			Number of optimal solutions		
		CP-8T	MIP_P2	MIP_P1	CP-8T	MIP_P2	MIP_P1	CP-8T	MIP_P2	MIP_P1
15	S	302.20	303.50	303.70	0.22	14.75	20.44	8	4	2
15	M	785.10	787.50	789.60	1.77	20.75	26.20	1	1	0
15	L	1543.20	1550.20	1551.80	1.62	17.14	22.55	2	3	3
20	S	416.90	423.00	426.20	2.79	51.88	58.09	0	0	0
20	M	1052.30	1063.90	1071.70	3.46	50.37	56.13	0	0	0
20	L	2121.70	2147.20	2157.30	3.55	53.58	59.01	0	0	0
25	S	541.80	554.80	559.20	2.91	68.23	71.78	0	0	0
25	M	1338.10	1360.10	1376.10	3.90	66.86	71.67	0	0	0
25	L	2595.50	2639.70	2670.50	3.90	67.69	71.29	0	0	0
40	S	850.10	885.10	906.70	3.21	81.41	84.97	0	0	0
40	M	2101.60	2167.80	2246.30	4.37	80.62	84.71	0	0	0
40	L	4229.40	4371.20	4475.90	4.40	81.21	84.80	0	0	0
50	S	1071.90	1117.70	1267.60	3.61	84.79	89.61	0	0	0
50	M	2608.80	NA	3059.00	4.30	NA	88.83	0	0	0
50	L	5353.70	NA	8373.60	4.81	NA	90.78	0	0	0
100	S	2233.00	NA	NA	4.25	NA	NA	0	0	0
100	M	5366.40	NA	NA	5.20	NA	NA	0	0	0
100	L	10748.70	NA	NA	5.51	NA	NA	0	0	0
Total		NA	NA	NA	NA	NA	NA	11	8	5
Mean		1457.68	1490.13	1523.28	3.05	56.87	61.64	NA	NA	NA

We notice from Table 4 that the CP-8T obtained the best metrics presented for all groups. Although the solver on the MIP_P2 struggled to find feasible solutions for larger instances, the MIP_P2

demonstrated superiority over the MIP_P1. Furthermore, the MIP_P2 outperformed the CP-8T in objective value in only two instances (each with 15 jobs), while the MIP_P1 did so in only one instance (also with 15 jobs). However, these differences are actually minimal in practice. Moreover, note that the number of optimal solutions in the group $15 \times L$ is three for the MIPs, and two for the CP-8T. Despite these few outliers, we conclude that the CP-8T is superior to the MIP formulations.

4.4. Comparison between our approaches and the best-known solutions

This section analyzes the performance of our main BRKGA approach (BRKGA-R-S-LS) and the CP-8T compared to the current best-known solutions (BKS). We consider the BKS as the best solution obtained by the MIP formulations and heuristics of [Khatami and Salehipour \(2024\)](#) (MIP_P1, MIP_P2, BS_P1, BS_P2, R&S), and our main approaches (CP-8T, BRKGA-R, BRKGA-R-S-LS). It is worth highlighting that we consider both the MIP solutions reported in the literature and those obtained in this work.

Figure 11 exhibits the distribution of RPD values for the BRKGA-R-S-LS compared to the BKS. The Relative Percentage Deviation (RPD) is calculated as $100 \cdot \frac{obj^{run} - obj^{BKS}}{obj^{BKS}}$, where obj^{run} is the makespan obtained on a run of the BRKGA-R-S-LS, and obj^{BKS} is the makespan of the BKS. Additionally, each box plot contains ten observations for each of the 30 instances with the same number of jobs n , totaling 300 observations per box plot. We observe that at least approximately 75% of the RPD values are at most 2.5%. Besides, apart from the groups with five, 40, and 50 jobs, no other group had outliers, and there are no significant differences between the medians, although it indicates a reduction as the number of jobs increases from $n \geq 40$. Therefore, these results indicate that the BRKGA-R-S-LS is a stable metaheuristic for this problem, obtaining high-quality approximate solutions within low computational times.

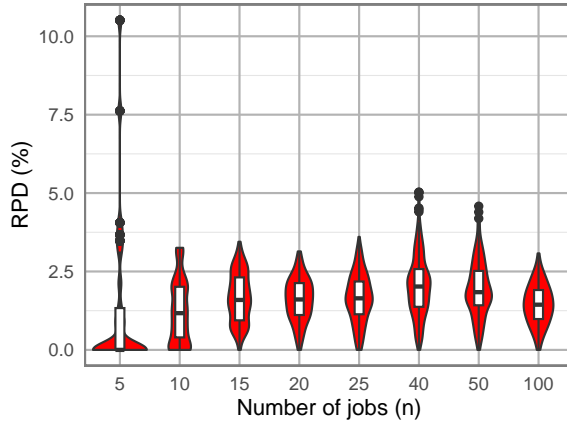


Figure 11: Distribution of RPD values for the BRKGA-R-S-LS compared to the BKS

Table 5 presents an overview of the CP-8T results in comparison with BKS for $n \geq 15$ (see Section 4.3), grouped by their number of jobs n and their category `cat`. Column `=BKS` shows the number of instances in which CP-8T obtained the BKS value. Column `opt` displays the number of proven optimal solutions found by CP-8T. Column `RPD (%)` exhibits the mean RPD value from the BKS, calculated as: $100 \cdot \frac{obj^{CP-8T} - obj^{BKS}}{obj^{BKS}}$, where obj^{CP-8T} is the objective value of the CP-8T, and obj^{BKS} is the objective

value of the BKS. Column **gap (%)** shows the mean gap value of the solver, i.e., $gap = 100 \cdot \frac{|bound-value|}{value}$, where *bound* is the objective bound, and *value* is the objective value. The row **Total** summarizes the results of all the instances by summing the columns. The row **Mean** summarizes the results of all the instances by taking the mean of the columns.

Table 5: Overview of the CP-8T results in comparison with the BKS

n	cat	=BKS	opt	RPD \pm std (%)	gap \pm std (%)
15	S	10	8	0.00 \pm 0.00	0.22 \pm 0.59
	M	9	1	0.06 \pm 0.18	1.77 \pm 1.07
	L	9	2	0.01 \pm 0.02	1.62 \pm 1.28
20	S	7	0	0.14 \pm 0.24	2.78 \pm 0.49
	M	10	0	0.00 \pm 0.00	3.46 \pm 0.16
	L	10	0	0.00 \pm 0.00	3.55 \pm 0.34
25	S	9	0	0.02 \pm 0.05	2.91 \pm 0.54
	M	9	0	0.03 \pm 0.09	3.89 \pm 0.28
	L	8	0	0.07 \pm 0.18	3.90 \pm 0.44
40	S	10	0	0.00 \pm 0.00	3.21 \pm 0.49
	M	7	0	0.14 \pm 0.28	4.37 \pm 0.90
	L	9	0	0.03 \pm 0.09	4.40 \pm 0.61
50	S	10	0	0.00 \pm 0.00	3.61 \pm 0.40
	M	8	0	0.07 \pm 0.15	4.30 \pm 0.46
	L	10	0	0.00 \pm 0.00	4.81 \pm 0.42
100	S	10	0	0.00 \pm 0.00	4.25 \pm 0.34
	M	9	0	0.05 \pm 0.17	5.21 \pm 0.42
	L	9	0	0.04 \pm 0.14	5.51 \pm 0.39
Total		163	11	—	—
Mean		—	—	0.04 \pm 0.13	3.54 \pm 1.41

We notice from Table 5 that the CP-8T reached the BKS value for 163 out of the 180 instances (90.56%). Regarding optimality, the CP-8T obtained optimal solutions for 11 out of the 180 instances (6.11%), all containing 15 jobs. The RPD value is only 0.04% on average with a standard deviation of 0.13%, i.e., despite the CP-8T not obtaining the BKS in some instances, the solution values obtained are similar. Finally, the solver gap is only 3.54% on average with a standard deviation of 1.41%, reaching a maximum average gap of 5.51% with a standard deviation of 0.39% for the group 100 x L.

4.5. Comparison between our proposed approaches

This section evaluates the proposed approaches by comparing their performance regarding solution quality given the same computational environment. Hence, we only consider the following approaches: BRKGA-R, BRKGA-R-S-LS, and CP-1T (see Section 4.2). Moreover, this analysis encompasses all the 240 instances of the benchmark, given that the three selected approaches did not obtain the optimal solution for all the instances with up to ten jobs.

Figure 12 depicts a distribution of the RPD values for two subsets of the benchmark, where each violin plot has a bandwidth equal to 0.25. The RPD is calculated as $100 \cdot \frac{obj^{run} - obj^{best}}{obj^{best}}$, where obj^{run} is the makespan obtained on a run of an approach and obj^{best} is the best makespan found across the three approaches. The graphics in Figure 12(a) consider the distributions for all 240 benchmark instances. The categories BRKGA-R and BRKGA-R-S-LS contain one observation for each of the ten independent runs, totaling 240 observations. Conversely, category CP-1T contains 240 observations, given

that the CP-1T was executed only once for each instance. Comparison of the medians indicates the superior performance of BRKGA-R-S-LS. Furthermore, CP-1T indicated the highest elongated distribution, suggesting inconsistent performance. In contrast, BRKGA-R-S-LS had the narrowest distribution, establishing it as the most stable and robust method. The bump arising in the lower tail of the distributions indicates that although BRKGA-R-S-LS obtained the highest number of solutions equal to the best solution among the three approaches, many of these solutions were also obtained by the other approaches. Besides, we highlight the presence of outliers above 7.5% in categories BRKGA-R and BRKGA-R-S-LS.

Figure 12(b) filters the distribution of RPD values of the three approaches for the 180 instances with at least 15 jobs. Hence, there are 1800 observations for BRKGA-R and BRKGA-R-S-LS, and 180 observations for CP-1T. This filtered distribution emphasizes the superior performance of BRKGA-R-S-LS compared to BRKGA-R, and in particular to CP-1T. Notice that for at least 75% of the observations of BRKGA-R-S-LS, the RPDs were smaller than at least 75% of the observations of the other approaches. Furthermore, for all observations of BRKGA-R-S-LS, the RPDs were smaller than at least 50% of the observations of the CP-1T. For at least 75% of the observations of BRKGA-R, the RPDs were smaller than at least 50% of the RPDs of the CP-1T. Moreover, a direct comparison between Figures 12(a) and 12(b) shows that the bump in the lower tail of each category and the outliers in the BRKGAs disappeared in the filtered distribution. These facts suggest that many of the observations that obtained solutions equal to the best solution among the three approaches and the outliers of the BRKGAs were actually for instances with up to ten jobs.

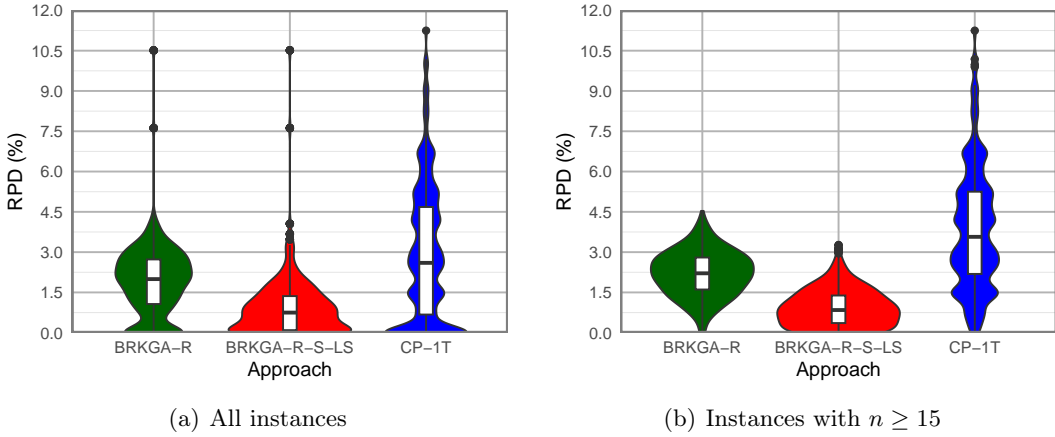


Figure 12: Distribution of RPD values of each approach.

4.6. Impact of the BRKGA components

In this section, we analyze the impact of the BRKGA-R-S-LS components. We executed some additional experiments considering two versions of the BRKGA that remove different BRKGA-R-S-LS components. The first, referred to as BRKGA with restarts and shakes (BRKGA-R-S), removes the local search component. The second, denoted as BRKGA with restarts and local search (BRKGA-R-LS), removes the shaking perturbation component. Moreover, the experiments were run on a small subset of the benchmark instances. This subset contains nine randomly selected instances, one for each variation on the number of jobs ($n \in \{25, 50, 100\}$) and categories (S, M, L). Furthermore, we performed ten

independent executions of the BRKGA-R-S and the BRKGA-R-LS for each instance. The results for the main approaches (BRKGA-R and BRKGA-R-S-LS) are the same as those reported in previous sections.

As for the main BRKGA approaches (BRKGA-R and BRKGA-R-S-LS), we employed the `irace` package to define the parameters of the BRKGA-R-S and the BRKGA-R-LS. Table 6 displays the parameter settings suggested by `irace`. Like the BRKGA-R-S-LS, we assume $r_{iLS} = n$ for the BRKGA-R-LS. Besides, we also assume $\gamma^{reset} \in \{\text{OB, BI, BMS}\}$. Finally, we highlight that setting $\gamma^{reset} = \text{CB}$ is equivalent to assuming $\gamma^{reset} = \text{OB}$ for the BRKGA-R-LS as well as for the BRKGA-R. For additional details concerning the parameters and configurations, see Appendix A.

Table 6: Settings suggested by `irace` for the set of experiments on the BRKGA-R-S and the BRKGA-R-LS.

Component	Notation	BRKGA-R-S		BRKGA-R-LS	
		Used	<code>irace</code>	Used	<code>irace</code>
Standard	n	✓	—	✓	—
	p	✓	187	✓	105
	p_e	✓	0.22	✓	0.35
	p_m	✓	0.10	✓	0.21
	ρ_e	✓	0.60	✓	0.68
Initial solution generator	α	✓	0.01	✓	0.03
	λ^{ws}	✓	0.90	✓	0.58
	n_{msi}	✓	679	✓	313
Perturbation	n_{nimp}	—	—	✓	144
	R	✓	141	—	—
	R^*	✓	5	—	—
	R^{**}	✓	9	—	—
	s^{type}	✓	CHANGE	—	—
	γ^{weak}	✓	CB	—	—
	γ^{strong}	✓	OB	—	—
	γ^{reset}	✓	BMS	✓	OB
Local search	b	—	—	✓	7
	L	—	—	✓	$0.18 \cdot n$
	r_{pLS}	—	—	✓	7
	r_{iLS}	—	—	✓	—

Figure 13 depicts the distribution of the RPD values for the nine instances selected, separated by each one of the four BRKGA approaches. Each violin plot has a bandwidth equal to 0.25. The RPD is calculated as: $100 \cdot \frac{obj^{run} - obj^{best}}{obj^{best}}$, where obj^{run} is the makespan achieved on a run of the respective BRKGA and obj^{best} is the best makespan acquired across the four approaches. Each violin plot contains 90 observations, one for each of the ten independent runs of the respective BRKGA on each of the nine instances. Notice that the medians decrease in the following order: BRKGA-R, BRKGA-R-S, BRKGA-R-LS, BRKGA-R-S-LS. Besides, observe that both the shaking and the local search components improve the solutions of the BRKGA-R, especially the local search component. Concerning the range of the RPD values, both the BRKGA-R-LS and the BRKGA-R-S-LS are generally competitive, although the bump arising in the lower tail of the BRKGA-R-S-LS distribution demonstrates the superiority of our main approach. Thereupon, the BRKGA components, combined or not, positively contribute to the quality of the BRKGA solutions.

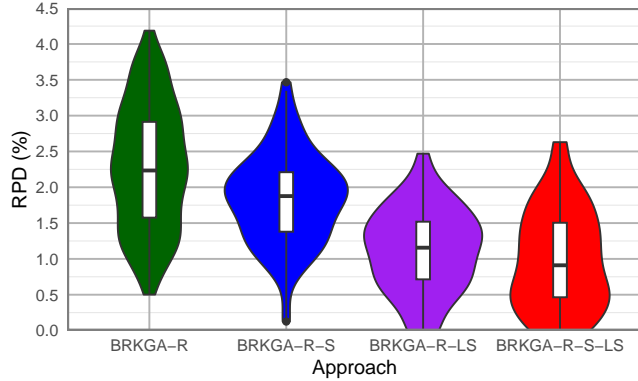


Figure 13: Impact of the BRKGA components.

5. Concluding remarks

In this paper, we considered the single-machine coupled task scheduling problem (SMCTSP) with exact delays to minimize the makespan. We proposed a constraint programming (CP) model and a biased random-key genetic algorithm (BRKGA) to tackle the problem. Our CP model applies well-established global constraints. Conversely, our BRKGA combines some successful components in the literature: an initial solution generator, periodical restarts and shakes, and a local search algorithm. To the best of our knowledge, this is the first time such approaches have been proposed in the context of coupled task scheduling.

The computational experiments indicate that the proposed approaches are promising for tackling the problem. We summarize the results only for the 180 instances with at least 15 jobs, which are the ones that were not all solved to optimality by the approaches in the literature. Concerning the exact formulations, the experiments show that the CP model outperformed the state-of-the-art MIP formulations, obtaining the smallest objective values, the smallest gaps, and the largest number of optimal solutions. Moreover, only the CP, compared to the MIP formulations, obtained feasible solutions for all the instances. Comparison between the tested approaches under the same computational settings, i.e., low time limit and one thread, indicated a superior performance of the BRKGA approach in terms of solution quality, compared to the CP model. Besides, the BRKGA approach acquired high-quality approximate solutions compared to the best known solutions within low computational times. The CP model with multiple threads and a longer running time of 3600 seconds obtained the best-known solution in 163 out of 180 (90.56%) of these instances. Finally, we show the importance of the shaking and local search components on the quality of our BRKGA solutions, especially the local search component.

Our study also tackled an undesirable behavior that may be faced with a BRKGA for certain problems, as was the case with the SMCTSP, which is a fast population homogeneity. We observed that some parameters of the BRKGA highly affect the population diversity through the generations. Hence, we adopted a *shaking* method. Instead of resetting the whole population, which fully destroys useful parts of the random-key vector that usually appear in better solutions, it controls the intensity of the modifications in the elite set and only resets the non-elite set. Combined with the injection of certain types of solution after each shake/reset, and a local search in selected situations, the resulting BRKGA significantly improved the overall solutions of the standard BRKGA with restarts.

Acknowledgments

This study was financed in part by the Coordenação de Aperfeiçoamento de Pessoal de Nível Superior - Brasil (CAPES) - Finance Code 001. This work was partially supported by the Brazilian National Council for Scientific and Technological Development (CNPq) research grants 314718/2023-0 and 445324/2024-4, and the FAPESB INCITE PIE0002/2022 grant.

References

Ageev, A.A., Baburin, A.E., 2007. Approximation algorithms for UET scheduling problems with exact delays. *Operations Research Letters* 35, 533–540.

Andrade, C.E., 2019. BrkgaMpIpr.jl. <https://github.com/ceandrade/BrkgaMpIpr.jl>. Last access: April 09, 2025.

Andrade, C.E., Silva, T., Pessoa, L.S., 2019. Minimizing flowtime in a flowshop scheduling problem with a biased random-key genetic algorithm. *Expert Systems with Applications* 128, 67–80.

Andrade, C.E., Toso, R.F., Gonçalves, J.F., Resende, M.G., 2021. The Multi-Parent Biased Random-Key Genetic Algorithm with Implicit Path-Relinking and its real-world applications. *European Journal of Operational Research* 289, 17–30.

Awad, M., Mulrennan, K., Donovan, J., Macpherson, R., Tormey, D., 2022. A constraint programming model for makespan minimisation in batch manufacturing pharmaceutical facilities. *Computers & Chemical Engineering* 156, 107565.

Bautista, M.G.A., Saganob, N.J., Concepcion, R., Bandala, A., Dadios, E., 2023. Automated cooking systems: Benefits, challenges, and future directions, in: 2023 IEEE 15th International Conference on Humanoid, Nanotechnology, Information Technology, Communication and Control, Environment, and Management (HNICEM), pp. 1–6. doi:[10.1109/HNICEM60674.2023.10589209](https://doi.org/10.1109/HNICEM60674.2023.10589209).

Bean, J.C., 1994. Genetic algorithms and random keys for sequencing and optimization. *ORSA Journal on Computing* 6, 154–160.

Békési, J., Dósa, G., Galambos, G., 2022. A first fit type algorithm for the coupled task scheduling problem with unit execution time and two exact delays. *European Journal of Operational Research* 297, 844–852.

Békési, J., Galambos, G., Jung, M.N., Oswald, M., Reinelt, G., 2014. A branch-and-bound algorithm for the coupled task problem. *Mathematical Methods of Operations Research* 80, 47–81.

Bessy, S., Giroudeau, R., 2019. Parameterized complexity of a coupled-task scheduling problem. *Journal of Scheduling* 22, 305–313.

Chaves, A., Gonçalves, J.F., Oliveira, R.M., Lorena, L.A., 2024. An adaptive biased random-key genetic algorithm for the tactical berth allocation problem, in: Proceedings of the 39th ACM/SIGAPP Symposium on Applied Computing, New York, NY, USA. p. 378–385. doi:[10.1145/3605098.3635993](https://doi.org/10.1145/3605098.3635993).

Condotta, A., Shakhlevich, N., 2014. Scheduling patient appointments via multilevel template: A case study in chemotherapy. *Operations Research for Health Care* 3, 129–144.

Condotta, A., Shakhlevich, N.V., 2012. Scheduling coupled-operation jobs with exact time-lags. *Discrete Applied Mathematics* 160, 2370–2388.

Da Col, G., Teppan, E.C., 2022. Industrial-size job shop scheduling with constraint programming. *Operations Research Perspectives* 9, 100249.

de Abreu, L.R., de Athayde Prata, B., Gomes, A.C., Braga-Santos, S.A., Nagano, M.S., 2022. A novel BRKGA for the customer order scheduling with missing operations to minimize total tardiness. *Swarm and Evolutionary Computation* 75, 101149.

den Besten, M., Stützle, T., 2001. Neighborhoods revisited: An experimental investigation into the effectiveness of variable neighborhood descent for scheduling, in: Proceedings of the 4th Metaheuristics International Conference, Porto, MIC 2001, pp. 545–549.

Festa, P., Guerriero, F., Resende, M.G.C., Scalzo, E., 2024. A biased random-key genetic algorithm with variable mutants to solve a vehicle routing problem. doi:[10.48550/arXiv.2405.00268](https://doi.org/10.48550/arXiv.2405.00268).

Fogel, D., 1994. An introduction to simulated evolutionary optimization. *IEEE Transactions on Neural Networks* 5, 3–14.

Gonçalves, J.F., Resende, M.G.C., 2011. Biased random-key genetic algorithms for combinatorial optimization. *Journal of Heuristics* 17, 487–525.

Hwang, F., Lin, B.M., 2011. Coupled-task scheduling on a single machine subject to a fixed-job-sequence. *Computers & Industrial Engineering* 60, 690–698.

Jiang, A.Z., Zhou, M., 2022. Design of Affordable Self-learning Home Cooking Robots, in: 2022 IEEE International Conference on Networking, Sensing and Control (ICNSC), pp. 1–6. doi:[10.1109/ICNSC55942.2022.10004056](https://doi.org/10.1109/ICNSC55942.2022.10004056).

Khatami, M., Salehipour, A., 2021. A binary search algorithm for the general coupled task scheduling problem. *4OR* 19, 593–611.

Khatami, M., Salehipour, A., 2024. The coupled task scheduling problem: an improved mathematical program and a new solution algorithm. *International Transactions in Operational Research* 31, 2399–2426.

Khatami, M., Salehipour, A., Cheng, T., 2019. Data for “Coupled task scheduling with exact delays: Literature review and models”. doi:[10.17632/dd7ht5k5pn.1](https://doi.org/10.17632/dd7ht5k5pn.1). v1.

Khatami, M., Salehipour, A., Cheng, T., 2020. Coupled task scheduling with exact delays: Literature review and models. *European Journal of Operational Research* 282, 19–39.

Kim, E.S., Lee, I.S., 2024. Heuristic approaches for scheduling of a two-machine flowshop with outsourcing lead-time. *Engineering Optimization* 56, 2431–2449.

Li, H., Zhao, H., 2007. Scheduling coupled-tasks on a single machine, in: 2007 IEEE Symposium on Computational Intelligence in Scheduling, IEEE. pp. 137–142.

Liu, Z., Lu, J., Liu, Z., Liao, G., Zhang, H.H., Dong, J., 2019. Patient scheduling in hemodialysis service. *Journal of Combinatorial Optimization* 37, 337–362.

Londe, M.A., Andrade, C.E., Pessoa, L.S., 2021. An evolutionary approach for the p-next center problem. *Expert Systems with Applications* 175, 114728.

Londe, M.A., Andrade, C.E., Pessoa, L.S., 2022. Exact and heuristic approaches for the root sequence index allocation problem. *Applied Soft Computing* 130, 109634.

Londe, M.A., Pessoa, L.S., Andrade, C.E., Resende, M.G., 2025. Biased random-key genetic algorithms: A review. *European Journal of Operational Research* 321, 1–22.

Londe, M.A., Pessoa, L.S., Andrade, C.E., Resende, M.G.C., 2024. Early years of biased random-key genetic algorithms: a systematic review. *Journal of Global Optimization* doi:[10.1007/s10898-024-01446-5](https://doi.org/10.1007/s10898-024-01446-5).

Lunardi, W.T., Birgin, E.G., Laborie, P., Ronconi, D.P., Voos, H., 2020. Mixed integer linear programming and constraint programming models for the online printing shop scheduling problem. *Computers & Operations Research* 123, 105020.

López-Ibáñez, M., Dubois-Lacoste, J., Pérez Cáceres, L., Stützle, T., Birattari, M., 2016. The irace package: Iterated racing for automatic algorithm configuration. *Operations Research Perspectives* 3, 43–58.

Martarelli, N.J., Nagano, M.S., 2020. Unsupervised feature selection based on bio-inspired approaches. *Swarm and Evolutionary Computation* 52, 100618.

Mauri, G.R., Biajoli, F.L., Raballo, R.L., Chaves, A.A., Ribeiro, G.M., Lorena, L.A.N., 2021. Hybrid metaheuristics to solve a multiproduct two-stage capacitated facility location problem. *International Transactions in Operational Research* 28, 3069–3093.

Melo, R.A., Ribeiro, C.C., Riveaux, J.A., 2023. A biased random-key genetic algorithm for the minimum quasi-clique partitioning problem. *Annals of Operations Research* 351, 575–607.

Mepani, M.M., Gala, K.B., Mishra, T.A., Suresh Bhole, K., Gholave, J., Daingade, S., 2022. Design of robot arm for domestic culinary assistance. *Materials Today: Proceedings* 68, 1930–1945. 4th International Conference on Advances in Mechanical Engineering.

Nethercote, N., Stuckey, P.J., Becket, R., Brand, S., Duck, G.J., Tack, G., 2007. MiniZinc: Towards a Standard CP Modelling Language, in: Bessière, C. (Ed.), *Principles and Practice of Constraint Programming – CP 2007*, Springer Berlin Heidelberg, Berlin, Heidelberg. pp. 529–543.

Orman, A.J., Potts, C.N., 1997. On the complexity of coupled-task scheduling. *Discrete Applied Mathematics* 72, 141–154.

Pandey, H.M., Chaudhary, A., Mehrotra, D., 2014. A comparative review of approaches to prevent premature convergence in GA. *Applied Soft Computing* 24, 1047–1077.

Pérez, E., Ntaimo, L., Wilhelm, W.E., Bailey, C., McCormack, P., 2011. Patient and resource scheduling of multi-step medical procedures in nuclear medicine. *IIE Transactions on Healthcare Systems Engineering* 1, 168–184.

Perron, L., Didier, F., 2024. CP-SAT Solver. URL: https://developers.google.com/optimization/cp/cp_solver/. last access: April 09, 2025.

Reixach, J., Blum, C., Djukanović, M., Raidl, G.R., 2025. A Biased Random Key Genetic Algorithm for Solving the Longest Common Square Subsequence Problem. *IEEE Transactions on Evolutionary Computation* 29, 390–403.

Rossi, F., van Beek, P., Walsh, T., 2006. *Handbook of Constraint Programming*. Elsevier Science Inc., USA.

Shapiro, R.D., 1980. Scheduling coupled tasks. *Naval Research Logistics Quarterly* 27, 489–498.

Sharma, K., Reddy, S.R.N., 2025. Design of smart automated cooker_a survey and feasibility study. *Multimedia Tools and Applications* 84, 18373–18394.

Sherali, H.D., Smith, J.C., 2005. Interleaving two-phased jobs on a single machine. *Discrete Optimization* 2, 348–361.

Silva, M.C., Melo, R.A., Resende, M.G., Santos, M.C., Toso, R.F., 2024. Obtaining the grundy chromatic number: How bad can my greedy heuristic coloring be? *Computers & Operations Research* 168, 106703.

Silva, M.C., Melo, R.A., Resende, M.G., Santos, M.C., Toso, R.F., 2025. The connected Grundy coloring problem: Formulations and a local-search enhanced biased random-key genetic algorithm. *Computers & Operations Research* 183, 107136.

Silva, S.E., Ribeiro, C.C., dos Santos Souza, U., 2023. A biased random-key genetic algorithm for the chordal completion problem. *RAIRO - Operations Research* 57, 1559–1578.

Spears, W., De Jong, K.A., 1991. On the virtues of parameterized uniform crossover, in: Belew, R., Booker, L. (Eds.), *Proceedings of the Fourth International Conference on Genetic Algorithms*, Morgan Kaufman, San Mateo. pp. 230–236.

Stuckey, P.J., Feydy, T., Schutt, A., Tack, G., Fischer, J., 2014. The MiniZinc Challenge 2008–2013. *AI Magazine* 35, 55–60.

Whitley, D., Rana, S., Heckendorn, R.B., 1999. The island model genetic algorithm: On separability, population size and convergence. *Journal of Computing and Information Technology* 7, 33–47.

Yi, J.s., Luong, T.A., Chae, H., Ahn, M.S., Noh, D., Tran, H.N., Doh, M., Auh, E., Pico, N., Yumbla, F., Hong, D., Moon, H., 2022. An Online Task-Planning Framework Using Mixed Integer Programming for Multiple Cooking Tasks Using a Dual-Arm Robot. *Applied Sciences* 12, 4018.

A. Parameter settings

This section details our process of parameter selection for the BRKGA. Recall that both BRKGA approaches have many parameters, especially BRKGA-R-S-LS. Thus, instead of performing a full factorial design, we used the `irace` package (López-Ibáñez et al., 2016) version 4.2.0 implemented in R, which provides an automatic configuration tool for tuning optimization algorithms. According to López-Ibáñez et al. (2016), this software package implements the *iterated racing*, a method that consists of three steps: (1) sampling new configurations according to a particular distribution; (2) selecting the best configurations from the newly sampled ones by means of racing; and (3) updating the sampling distribution to bias the sampling towards the best configurations. These three steps are repeated until a termination criterion is met.

For this task, we generated a new training set of instances for parametrization according to the general benchmark set proposed in Khatami et al. (2019, 2020), using Python 3.11.9. This new set contains 24 instances, two for each of the three categories and four different numbers of jobs, i.e., $n \in \{15, 25, 50, 100\}$. In total, there are 24 instances. We defined a block of instances of size four, which contains instances of the same category for each value of n . This means that `irace` will only eliminate a configuration after evaluating a complete block and never in the middle of the block. We also run the `irace` for each BRKGA approach, being that we used a budget of 4000 experiments for the BRKGA-R, 5000 experiments for both BRKGA-R-S and BRKGA-R-LS, and 6000 experiments for the BRKGA-R-S-LS, given that it contains more parameters. The remaining `irace` parameters were configured according to the default settings.

Table 7 exhibits the ranges used to tune the BRKGA parameters using `irace`. Recall Sections 3.4 and 4.2 for the meaning of the notations OB (overall best), CB (current best), BI (best initial solution), and BMS (best multi-start). Besides, we forbid $R^{**} < R^*$ and the maximum number of digits of the real numbers is two. Finally, the parameter L in the local search component was set to be proportional to n , i.e., $L = \lambda^{pLS} \cdot n$, where $\lambda^{pLS} \in [0, 1]$ is the percentage of the number of jobs that defines the frequency of the periodic LS. In this way, the greater the number of jobs, the lower the frequency of the periodic LS. This aimed at reducing the total time spent in LS.

Tables 8-11 exhibit the best configurations provided by `irace` for the BRKGA-R, BRKGA-R-S, BRKGA-R-LS, and BRKGA-R-S-LS, listed from best to worst.

Table 7: Ranges used to tune the BRKGA parameters using `irace`

Component	Notation	BRKGA-R	BRKGA-R-S	BRKGA-R-LS	BRKGA-R-S-LS
Standard	p	$\mathbb{Z} \cap [100, 200]$	$\mathbb{Z} \cap [100, 200]$	$\mathbb{Z} \cap [100, 200]$	$\mathbb{Z} \cap [100, 200]$
	p_e	$\mathbb{R} \cap [0.10, 0.50]$	$\mathbb{R} \cap [0.10, 0.50]$	$\mathbb{R} \cap [0.10, 0.50]$	$\mathbb{R} \cap [0.10, 0.50]$
	p_m	$\mathbb{R} \cap [0.10, 0.50]$	$\mathbb{R} \cap [0.10, 0.50]$	$\mathbb{R} \cap [0.10, 0.50]$	$\mathbb{R} \cap [0.10, 0.50]$
	ρ_e	$\mathbb{R} \cap [0.50, 0.80]$	$\mathbb{R} \cap [0.50, 0.80]$	$\mathbb{R} \cap [0.50, 0.80]$	$\mathbb{R} \cap [0.50, 0.80]$
Initial solution generator	α	$\mathbb{R} \cap [0.00, 0.10]$	$\mathbb{R} \cap [0.00, 0.10]$	$\mathbb{R} \cap [0.00, 0.10]$	$\mathbb{R} \cap [0.00, 0.10]$
	λ^{ws}	$\mathbb{R} \cap [0.05, 1.00]$	$\mathbb{R} \cap [0.05, 1.00]$	$\mathbb{R} \cap [0.05, 1.00]$	$\mathbb{R} \cap [0.05, 1.00]$
	n_{msi}	$\mathbb{Z} \cap [300, 1500]$	$\mathbb{Z} \cap [300, 1500]$	$\mathbb{Z} \cap [300, 1500]$	$\mathbb{Z} \cap [300, 1500]$
Perturbation	n_{nimp}	$\mathbb{Z} \cap [50, 1000]$	—	$\mathbb{Z} \cap [50, 1000]$	—
	R	—	$\mathbb{Z} \cap [50, 250]$	—	$\mathbb{Z} \cap [50, 250]$
	R^*	—	$\mathbb{Z} \cap [2, 5]$	—	$\mathbb{Z} \cap [2, 5]$
	R^{**}	—	$\mathbb{Z} \cap [3, 10]$	—	$\mathbb{Z} \cap [3, 10]$
	s^{type}	—	{CHANGE, SWAP}	—	{CHANGE, SWAP}
	γ^{weak}	—	{CB, OB}	—	{CB, OB}
	γ^{strong}	—	{OB, BMS}	—	{OB, BMS}
	γ^{reset}	{OB, BI, BMS}	{OB, BMS}	{OB, BI, BMS}	{OB, BMS}
Local search	b	—	—	$\mathbb{Z} \cap [1, 10]$	$\mathbb{Z} \cap [1, 10]$
	L	—	—	$\mathbb{R} \cap [0.10, 0.50] \cdot n$	$\mathbb{R} \cap [0.10, 0.50] \cdot n$
	r_{pLS}	—	—	$\mathbb{Z} \cap [2, 7]$	$\mathbb{Z} \cap [2, 7]$

Table 8: `irace` results for BRKGA-R, listed from best to worst

Standard				Initial solution generator			Perturbation	
p	p_e	p_m	ρ_e	α	λ^{ws}	n_{msi}	n_{nimp}	γ^{reset}
163	0.39	0.20	0.74	0.02	0.28	1374	956	BMS
166	0.47	0.14	0.73	0.03	0.53	1339	859	BMS
164	0.39	0.14	0.65	0.01	0.57	1222	568	BMS
149	0.43	0.25	0.74	0.01	0.35	1144	879	BMS
144	0.39	0.22	0.75	0.03	0.23	1185	974	BMS

Table 9: `irace` results for BRKGA-R-S, listed from best to worst

Standard				Initial solution generator			Perturbation						
p	p_e	p_m	ρ_e	α	λ^{ws}	n_{msi}	R	R^*	R^{**}	s^{type}	γ^{weak}	γ^{strong}	γ^{reset}
187	0.22	0.10	0.60	0.01	0.90	679	141	5	9	CHANGE	CB	OB	BMS
145	0.24	0.10	0.68	0.02	0.90	891	206	3	9	CHANGE	CB	OB	BMS

Table 10: `irace` results for BRKGA-R-LS, listed from best to worst

Standard				Initial solution generator			Perturbation		Local search		
p	p_e	p_m	ρ_e	α	λ^{ws}	n_{msi}	n_{nimp}	γ^{reset}	b	L	r_{pLS}
105	0.35	0.21	0.68	0.03	0.58	313	144	OB	7	0.18	7
108	0.40	0.25	0.72	0.04	0.62	433	143	OB	8	0.24	7
182	0.30	0.19	0.69	0.02	0.33	1044	127	OB	7	0.28	7
195	0.43	0.17	0.72	0.02	0.08	1475	257	OB	7	0.30	7

Table 11: `irace` results for BRKGA-R-S-LS, listed from best to worst

Standard				Initial solution generator			Perturbation					Local search				
p	p_e	p_m	ρ_e	α	λ^{ws}	n_{msi}	R	R^*	R^{**}	s^{type}	γ^{weak}	γ^{strong}	γ^{reset}	b	L	r_{pLS}
185	0.43	0.24	0.78	0.01	0.22	602	154	2	9	SWAP	OB	OB	OB	9	0.21	7
180	0.39	0.14	0.79	0.04	0.88	1281	121	4	10	CHANGE	CB	BMS	OB	10	0.13	6
164	0.43	0.11	0.70	0.05	0.27	1156	155	3	4	SWAP	OB	OB	OB	9	0.24	7
191	0.37	0.18	0.74	0.02	0.13	649	218	2	4	SWAP	OB	OB	OB	9	0.19	7
154	0.39	0.19	0.74	0.02	0.57	1299	98	5	8	CHANGE	CB	BMS	OB	7	0.17	6
197	0.45	0.14	0.77	0.01	0.11	523	159	2	6	SWAP	OB	OB	OB	9	0.14	7

B. Population homogeneity in the BRKGA

In this section, we illustrate a fact observed during preliminary analysis regarding the percentage of unique random-key vectors in a population throughout the generations. To accomplish that, we selected the instance 100_2_L_gen from the general set of Khatami et al. (2019, 2020)'s benchmark. Figure 14 depicts the effect of p_e , p_m , and ρ_e on BRKGA-R's diversity and solution improvement. For each population generation, the left axis shows the uniqueness percentage of the random-key vectors and the sequences of jobs. Conversely, the right axis presents the evolution of the overall best solution in each generation. We consider $p = 150$, $n_{nimp} = 1000$, $\alpha = 0.05$, $\lambda^{ws} = 0.12$, $n_{msi} = 1000$, and $\gamma^{reset} = \text{OB}$.

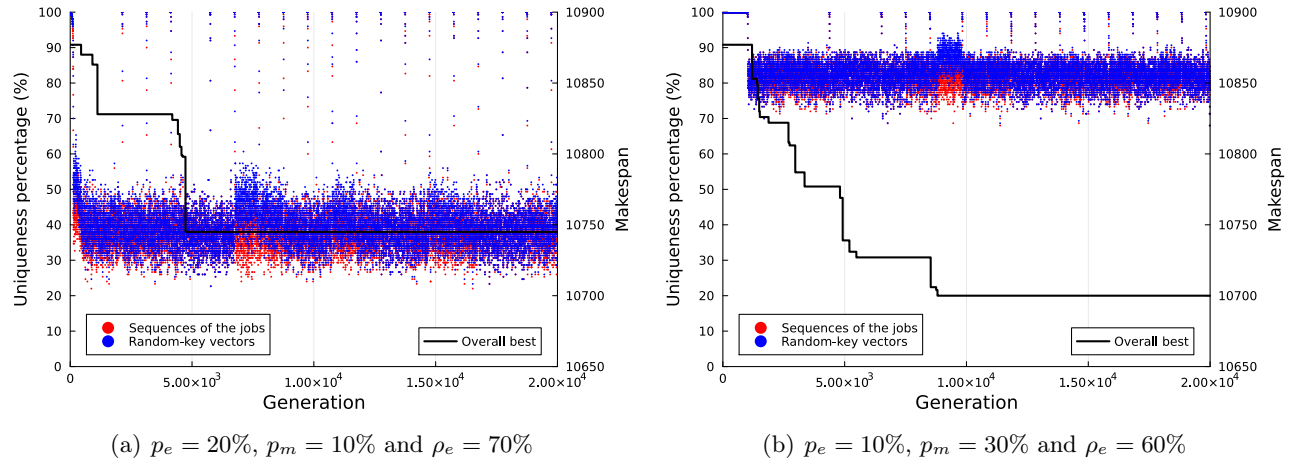


Figure 14: Effect of p_e , p_m , and ρ_e on BRKGA-R's population diversity and solution improvement. Instance 100_2_L_gen.

Observe that Figures 14(a) and 14(b) indicate that higher elite percentages p_e , lower mutant percentages p_m , and higher inheritance probability of elite parent key ρ_e lead to a less diverse population. Note that both configurations quickly converged to the same uniqueness percentage range after each reset. Besides, in Figure 14(b) the uniqueness percentage did not converge before the first restart, which indicates that the percentage of warm-start solutions in the initial population also affected the convergence's velocity. Furthermore, both plots indicate that several new series of improvement start a few generations after a new reset, particularly after a convergence. Moreover, small key changes may not increase diversification as different random-key vectors convert to the same sequence when sorted. Although the scenario presented in Figure 14(a) may be undesirable, it is not clear that the configuration of Figure 14(b) provides better results.

In Figure 14(b), we increased population diversity by setting a lower p_e , a higher p_m , and a lower ρ_e . However, this figure does not depict whether these non-unique random-key vectors are concentrated in a few individuals or spread across the whole population. Figure 15 deepens the analysis of the BRKGA-R's diversity in the elite set for the same runs of Figure 14. Observe that both configurations still resulted in homogeneous elite sets. This situation is even more evident regarding the uniqueness percentage of the job's sequences. Hence, modifying the parameters p_e , p_m , and ρ_e may not be sufficient for generating a diverse population, particularly in the elite set.

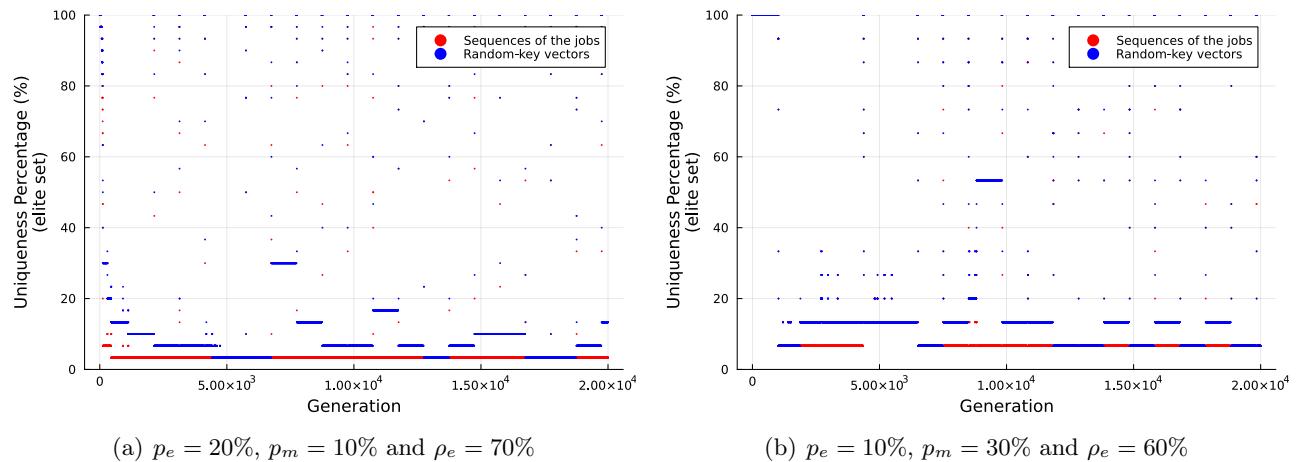


Figure 15: Effect of p_e , p_m , and ρ_e on BRKGA-R's elite set diversity. Instance 100_2_L_gen.